

# Stabilizing Sharpness-aware Minimization Through A Simple Renormalization Strategy

**Chengli Tan**

*School of Mathematics and Statistics  
Xi'an Jiaotong University  
Xi'an, 710049, China*

CLTAN023@OUTLOOK.COM

**Jiangshe Zhang**

*School of Mathematics and Statistics  
Xi'an Jiaotong University  
Xi'an, 710049, China*

JSZHANG@MAIL.XJTU.EDU.CN

**Junmin Liu**

*School of Mathematics and Statistics  
Xi'an Jiaotong University  
Xi'an, 710049, China*

JUNMINLIU@MAIL.XJTU.EDU.CN

**Yicheng Wang**

*School of Mathematics and Statistics  
Xi'an Jiaotong University  
Xi'an, 710049, China*

YCWANG@STU.XJTU.EDU.CN

**Yunda Hao**

*Department of Machine Learning  
Centrum Wiskunde & Informatica  
Amsterdam, 1098 XG, the Netherlands*

YUNDA@CWI.NL

**Editor:** N/A

## Abstract

Recently, sharpness-aware minimization (SAM) has attracted a lot of attention because of its surprising effectiveness in improving generalization performance. However, training neural networks with SAM can be highly unstable since the loss does not decrease along the direction of the *exact gradient* at the current point, but instead follows the direction of a *surrogate gradient* evaluated at another point nearby. To address this issue, we propose a simple renormalization strategy, dubbed StableSAM, so that the norm of the surrogate gradient maintains the same as that of the exact gradient. Our strategy is easy to implement and flexible enough to integrate with SAM and its variants, almost at no computational cost. With elementary tools from convex optimization and learning theory, we also conduct a theoretical analysis of sharpness-aware training, revealing that compared to stochastic gradient descent (SGD), the effectiveness of SAM is only assured in a limited regime of learning rate. In contrast, we show how StableSAM extends this regime of learning rate and when it can consistently perform better than SAM with minor modification. Finally, we demonstrate the improved performance of StableSAM on several representative data sets and tasks.

**Keywords:** Deep neural networks, sharpness-aware minimization, expected risk analysis, uniform stability, stochastic optimization

## 1. Introduction

Over the last decade, deep neural networks have been successfully deployed in a variety of domains, ranging from object detection (Redmon et al., 2016), machine translation (Dai et al., 2019), to mathematical reasoning (Davies et al., 2021), and protein folding (Jumper et al., 2021). Generally, deep neural networks are applied to approximate an underlying function that fits the training set well. In the realm of supervised learning, this is equivalent to solving an unconstrained optimization problem

$$\min_{\mathbf{w}} F_S(\mathbf{w}) \triangleq \frac{1}{n} \sum_{i=1}^n f(\mathbf{w}, z_i), \quad (1)$$

where  $f$  represents the per-example loss,  $\mathbf{w} \in \mathbb{R}^d$  denotes the parameters of the deep neural network, and  $n$  feature/label pairs  $z_i = (x_i, y_i)$  constitute the training set  $S$ . Often, we assume each example is i.i.d. generated from an unknown data distribution  $\mathcal{D}$ . Minimizing the empirical risk in (1) is quite challenging, since deep neural networks are composed of many non-linear layers and the number of learnable parameters often surpasses the number of training examples we can acquire, making the loss landscape highly dimensional and very complex.

In practice, due to the limited memory and time, we can not simultaneously store the gradients of each example in the training set and directly apply determined methods such as gradient descent to train deep neural networks. Instead, we use only a small subset (so-called mini-batch) of the training examples to estimate the exact gradient and then employ stochastic gradient-based methods to make training millions (even billions) of parameters feasible. However, the generalization ability of the solutions can vary with different training hyperparameters and optimizers. For example, Jastrzbski et al. (2018); Keskar et al. (2017); He et al. (2019) argued that training neural networks with a larger ratio of learning rate to mini-batch size tends to find solutions that generalize better. Meanwhile, Wilson et al. (2017); Zhou et al. (2020) also pointed out that the solutions found by adaptive optimization methods such as Adam (Kingma and Ba, 2014) and AdaGrad (Duchi et al., 2011) often generalize significantly worse than SGD (Bottou et al., 2018). Although the relationship between stochastic optimizer and generalizability remains not fully understood (Choi et al., 2019; Dahl et al., 2023), it is generally appreciated that solutions recovered from the flat regions of the loss landscape generalize better than those landing in sharp regions (Keskar et al., 2017; Chaudhari et al., 2019; Kaddour et al., 2022). This can be justified from the perspective of the minimum description length principle that fewer bits of information are required to describe a flat minimum (Hinton and van Camp, 1993), which, as a result, leads to stronger robustness against distribution shift between training data and test data.

Based on this observation, different approaches are proposed towards finding flatter minima, amongst which the sharpness-aware minimization (SAM) (Foret et al., 2021) substantially improves the generalizability and attains state-of-art results on training large-scale models such as vision transformers (Chen et al., 2022) and language models (Bahri et al., 2022). However, training neural networks with SAM and its variants can be highly unstable (Kwon et al., 2021; Yue et al., 2023; Kim et al., 2023) and thus requires particular attention on hyperparameter tuning. Different from standard training that uses the *exact gradient* at the current point to update  $\mathbf{w}$ , SAM uses a *surrogate gradient* evaluated at the perturbed

Table 1: Comparative results on expected excess risk of different optimization methods. Note that our discussion is focused on the  $\mu$ -strongly convex problems and the loss function is assumed to be  $G$ -Lipschitz continuous and  $L$ -smooth. The constant  $\rho > 0$  indicates the perturbation radius of SAM and  $\gamma_0, \gamma_1, C$  are arbitrary constants so that  $0 < \gamma_0 \leq \gamma_1 < 1$  and  $C > 1$ .

	Expected Excess Risk	Learning Rate
SGD	$\varepsilon_{exc} \leq \frac{2G^2(\mu+L)}{n\mu L} + \frac{\eta G^2 L}{4\mu}$	$\eta \leq \frac{2}{\mu+L}$
SAM (Theorem 11)	$\varepsilon_{exc} \leq \frac{2G^2(\mu+L)}{n\mu L(1+\mu\rho/G)} + \frac{\eta G^2 L}{4\mu(1+\mu\rho/G)}$	$\eta \leq \frac{2}{\mu+L} \frac{1+\mu\rho/G}{(1+CL\rho/G)^2}$
StableSAM (Theorem 18)	$\varepsilon_{exc} \leq \frac{2\gamma_1 G^2(\mu+L)}{n\mu L(1+\mu\rho/G)} + \frac{\eta \gamma_1^2 G^2 L}{4\gamma_0 \mu(1+\mu\rho/G)}$	$\eta \leq \frac{2}{\mu+L} \frac{1+\mu\rho/G}{\gamma_1(1+CL\rho/G)^2}$

\* Risk analysis of SGD can be easily inferred from Hardt et al. (2016) using known results.

weight  $\mathbf{w}^{asc}$  to update it. This unusual operation incurs instability in the training process: On one hand, using a surrogate gradient to update the parameters does not necessarily promise to decrease the training loss in expectation, though possibly flatter regions might be explored (Zhuang et al., 2022); on the other hand, the surrogate gradient norm at location  $\mathbf{w}^{asc}$ ,  $\|\nabla f(\mathbf{w}^{asc})\|_2$ , is generally much larger than the exact gradient norm at  $\mathbf{w}$ ,  $\|\nabla f(\mathbf{w})\|_2$  (see Figure 1).

To stabilize training neural networks with SAM and its variants, here we propose a simple yet effective strategy by rescaling the gradient norm at point  $\mathbf{w}^{asc}$  to the same magnitude as the gradient norm at point  $\mathbf{w}$ . In brief, our contributions can be summarized as follows:

1. We proposed a simple strategy, dubbed StableSAM, to stabilize training deep neural networks with SAM optimizer. Our strategy is easy to implement and flexible enough to be integrated with any other SAM variants, almost at no computational cost. Most importantly, our strategy does not introduce any additional hyperparameter, tuning which is quite time-consuming in the context of sharpness-based optimization.
2. We theoretically analyzed the benefits of SAM over SGD in terms of expected excess risk and found that the superiority of SAM is only assured in a limited regime of learning rate (see Table 1). We further extended the study to StableSAM and showed that it allows for a larger learning rate and can consistently perform better than SAM under some mild conditions.
3. We empirically validated the capability of StableSAM to stabilize sharpness-aware training and demonstrated its improved generalization performance in real-world problems.

The remainder of the study is organized as follows. Section 2 reviews the related literature, while Section 3 details the implementation of the renormalization strategy. Section 4 then provides a theoretical analysis of SAM and StableSAM from the perspective of uniform stability. Finally, before concluding the study, Section 5 presents the experimental results.

## 2. Related Works

Since the seminal work of SAM (Foret et al., 2021), many successive approaches have emerged, and most of them can be roughly grouped into two classes.

The first class aims to further improve the generalizability of SAM. For example, to strengthen the connection between sharpness and generalizability, which might break up due to model reparameterization, ASAM (Kwon et al., 2021) was proposed by stretching/shrinking the neighborhood ball according to the magnitude of parameters. Similarly, instead of defining the neighborhood ball in the Euclidean space, FisherSAM (Kim et al., 2022) runs the SAM update on the statistical manifold induced by the Fisher information. Since one-step gradient ascent may not suffice to accurately approximate the solution of the inner maximization, RSAM (Liu et al., 2022b) was put forward by smoothing the loss landscape with Gaussian filters. This approach is similar to Haruki et al. (2019); Bisla et al. (2022), both of which aim to flatten the loss landscape by convoluting the loss function with stochastic noise. To separate the goal of minimizing the training loss and sharpness, GSAM (Zhuang et al., 2022) was proposed to seek a region with both small loss and low sharpness. Contrary to finding a common weight perturbation within each mini-batch,  $\delta$ -SAM (Zhou et al., 2022) uses an approximate per-instance perturbation by dynamically reweighting perturbation with a theoretically principled weighting factor. Apart from being analyzed from the perspective of regularization (Zhao et al., 2022a; Zhang et al., 2023; Yue et al., 2023), different variants of SAM are further proposed to fit in model-agnostic (Li and Giannakis, 2023), class-imbalanced (Zhou et al., 2023), and parameter-corrupted (Zhang et al., 2022) settings.

Since SAM involves two gradient backpropagations at each iteration, it consequently doubles the computational cost than in standard training. So the second class strives to reduce the computation overhead while retaining the same generalizability as SAM. An early attempt is LookSAM (Liu et al., 2022a), which executes a SAM update every few iterations. Another simple strategy is RST (Zhao et al., 2022b), according to which SAM and standard training are randomly switched with a scheduled probability. ESAM (Du et al., 2022a) and SSAM (Mi et al., 2022) both attempt to perturb a subset of parameters to estimate the sharpness measure, while KSAM (Ni et al., 2022) only applies the SAM update to the examples with the highest loss. Another intriguing approach is SAF (Du et al., 2022b), which accelerates the training process by replacing the sharpness measure with a trajectory loss. However, this approach is heavily memory-consuming as it needs to store the outputs of each example in history.

In contrast to these studies, our approach concentrates on improving the training stability of sharpness-aware optimization, functioning as a plug-and-play component for SAM and its successors. Despite its simplicity, our approach is shown to be more robust with the large learning rates and can achieve similar or even superior generalization performance compared to the vanilla SAM.

## 3. Methodology

As formulated in (1), standard training focuses on minimizing the empirical risk of a single weight  $\mathbf{w}$  over the training set  $S$ . This training procedure tends to overfit the training set

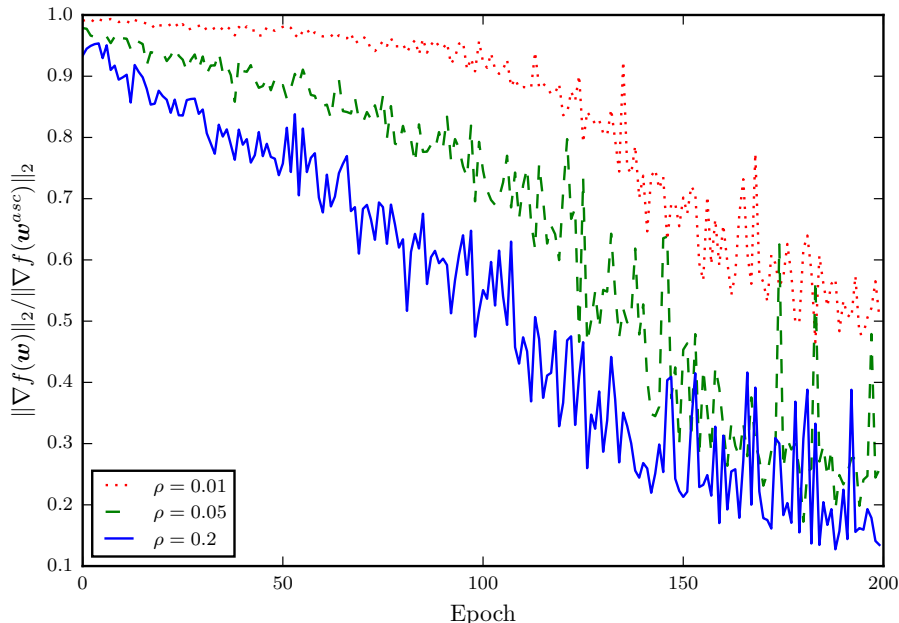


Figure 1: Evolution of the ratio of the norm of the exact gradient  $\nabla f(\mathbf{w})$  evaluated at current point  $\mathbf{w}$  to that of the surrogate gradient  $\nabla f(\mathbf{w}^{asc})$  evaluated at the perturbed weight  $\mathbf{w}_t^{asc}$ . The neural network, ResNet-18, is trained on an image training set CIFAR-100 up to 200 epochs using the SAM optimizer with different perturbation radius  $\rho \in \{0.01, 0.05, 0.2\}$ .

and as a result, converges to sharp minima. In contrast, SAM biases the training towards the flat regions of the loss landscape and seeks a neighborhood with low training losses such that small perturbations to the model weights do not significantly alter the generalization performance. To this end, SAM proposes to solve the following minimax problem:

$$\min_{\mathbf{w}} F_S^{SAM}(\mathbf{w}) \quad \text{where} \quad F_S^{SAM}(\mathbf{w}) \triangleq \max_{\|\epsilon\|_2 \leq \rho} F_S(\mathbf{w} + \epsilon),$$

where  $\rho > 0$  is a predefined constant controlling the radius of the neighborhood ball, and  $\epsilon \in \mathbb{R}^d$  is a random weight perturbation vector. In practice, due to the difficulty of solving the inner maximization problem, SAM optimizes the following objective function by a series of Taylor approximation

$$\min_{\mathbf{w}} F_S(\mathbf{w} + \tilde{\epsilon}), \quad \text{where} \quad \tilde{\epsilon} = \rho \nabla F_S(\mathbf{w}) / \|\nabla F_S(\mathbf{w})\|_2.$$

By first ascending the weights along the gradient direction and then evaluating the surrogate gradient at  $\mathbf{w}^{asc} = \mathbf{w} + \tilde{\epsilon}$ , SAM minimizes the ‘‘perturbed weights’’ with the highest loss within the neighborhood.

However, training deep neural networks with SAM sometimes is highly unstable, especially for models with drastic gradient changes (Zhang et al., 2022). This is because updating the parameters  $\mathbf{w}$  with a surrogate gradient evaluated at  $\mathbf{w}^{asc}$  does not assure a decreased training loss, and minimizing the perturbed loss  $F_S^{SAM}(\mathbf{w})$  does not promise the solutions

---

**Algorithm 1** StableSAM Optimizer

---

**Input:** Training set  $S = \{(x_i, y_i)\}_{i=1}^n$ , objective function  $F_S(\mathbf{w})$ , initial parameters  $\mathbf{w}_0 \in \mathbb{R}^d$ , learning rate  $\eta > 0$ , perturbation radius  $\rho > 0$ , training iterations  $T$ , and base optimizer  $\mathcal{A}$  (e.g. SGD)

**Output:**  $\mathbf{w}_T$

- 1: **for**  $t = 0, 1, \dots, T - 1$  **do**
  - 2:   Sample a mini-batch  $B_t = \{(x_{t_1}, y_{t_1}), \dots, (x_{t_b}, y_{t_b})\}$ ;
  - 3:   Compute exact gradient  $\mathbf{g}_t = \nabla_{\mathbf{w}} F_{B_t}(\mathbf{w})|_{\mathbf{w}=\mathbf{w}_t}$  of the loss over  $B_t$ ;
  - 4:   Compute perturbed weights  $\mathbf{w}_t^{asc} = \mathbf{w}_t + \rho \mathbf{g}_t / \|\mathbf{g}_t\|_2$ ;
  - 5:   Compute surrogate gradient  $\mathbf{g}_t^{asc} = \nabla_{\mathbf{w}} F_{B_t}(\mathbf{w})|_{\mathbf{w}=\mathbf{w}_t^{asc}}$  of the loss over the same  $B_t$ ;
  - 6:   **Renormalize surrogate gradient with**  $\mathbf{g}_t^{asc} = \frac{\|\mathbf{g}_t\|_2}{\|\mathbf{g}_t^{asc}\|_2} \mathbf{g}_t^{asc}$ ;
  - 7:   Update weights with base optimizer  $\mathcal{A}$  by  $\mathbf{w}_{t+1} = \mathbf{w}_t - \eta \mathbf{g}_t^{asc}$ ;
  - 8: **end for**
- 

found by SAM live in the flat regions of the loss landscape (Zhuang et al., 2022). Moreover, as depicted in Figure 1, the norm of the surrogate gradient at  $\mathbf{w}^{asc}$  is much larger than the norm of the exact gradient at  $\mathbf{w}$ , a problem that is particularly severe in the late stages of training. Despite the potential benefit of helping the optimizer escape from sharp valleys, it brings about the problem of gradient explosion in the early stages of training and of overshooting and oscillation in the late stages (Kim et al., 2023).

To address this issue, we propose a simple strategy, dubbed StableSAM, to improve the stability of sharpness-aware training. As shown in Algorithm 1<sup>1</sup>, the only difference from SAM is that we include an extra renormalization step (line 6) to ensure that the norm of the rescaled surrogate gradient  $\mathbf{g}_t^{asc}$  does not exceed that of the exact gradient  $\mathbf{g}_t$ . The coefficient,  $\|\mathbf{g}_t\|_2 / \|\mathbf{g}_t^{asc}\|_2$ , which we refer to as the *renormalization factor*, can be interpreted as follows. When  $\|\mathbf{g}_t^{asc}\|_2$  is larger than  $\|\mathbf{g}_t\|_2$ , it indicates that the perturbed weight  $\mathbf{w}^{asc}$  resides in a sharper region of the loss landscape and its gradient is more effective in helping the optimizer escape from saddle points. Therefore, we downscale the norm of  $\mathbf{g}_t^{asc}$  to prevent  $\mathbf{w}_t$  from moving too far and getting trapped in another saddle point. In contrast, when  $\|\mathbf{g}_t^{asc}\|_2$  is smaller than  $\|\mathbf{g}_t\|_2$ , a situation that rarely occurs though, it indicates that the perturbed weight  $\mathbf{w}^{asc}$  resides in a flatter region and its gradient is less effective in helping the optimizer escape from saddle points. In this case, we need to upscale the norm of  $\mathbf{g}_t^{asc}$  to incur a larger perturbation. Finally, it should be noted that our approach does not introduce any additional hyperparameter compared to the vanilla SAM.

## 4. Theoretical Analysis

Conventionally, the generalizability of sharpness-aware training is guaranteed by the PAC-Bayesian theory (Foret et al., 2021; Yue et al., 2023; Zhuang et al., 2022). This approach, however, is fundamentally limited since the generalization bound is focused on the worst-case perturbation rather than the realistic one-step ascent approximation (Wen et al., 2022). For a certain class of problems, an analysis from the perspective of implicit bias suggests that SAM can always choose a better solution than SGD (Andriushchenko and Flammarion,

---

1. A PyTorch implementation is available at <https://github.com/cltan023/stablesam2024>.

2022). Besides, Compagnoni et al. (2023) further characterized the continuous-time models (in the form of a stochastic differential equation) for SAM in the small learning rate regime and concluded that SAM is attracted to saddle points under some realistic conditions, an observation which has also been unveiled by Kim et al. (2023). Moreover, Bartlett et al. (2023) argued that SAM converges to a cycle that oscillates between the minimum along the principal direction of the Hessian. Different from these studies, here we investigate the generalization performance of SAM via *uniform stability* (Bousquet and Elisseeff, 2002) and together with its convergence properties present an upper bound over its expected excess risk. We first show that SAM consistently performs better than SGD, though a much smaller learning rate is required. Finally, we show how our proposed method, StableSAM, extends the regime of learning rate and when it can achieve a better generalization performance than SAM.

#### 4.1 Notations and Preliminaries

Let  $X \subset \mathbb{R}^p$  and  $Y \subset \mathbb{R}$  denote the feature and label space, respectively. We consider a training set  $S$  of  $n$  examples, each of which is randomly sampled from an unknown distribution  $\mathfrak{D}$  over the data space  $Z = X \times Y$ . Given a learning algorithm  $\mathcal{A}$ , it learns a hypothesis that relates the input  $x \in X$  to the output  $y \in Y$ . For deep neural networks, the learned hypothesis is parameterized by the network parameters  $\mathbf{w} \in \mathbb{R}^d$ . We further assume that the hypothesis learned by  $\mathcal{A}$  does not depend on the order of the elements in the training set  $S$ .

Suppose  $f(\mathbf{w}, z) : \mathbb{R}^d \times Z \mapsto \mathbb{R}_+$  is a non-negative cost function, we then can define the *population risk*

$$F_{\mathfrak{D}}(\mathbf{w}) \triangleq \mathbb{E}_{z \sim \mathfrak{D}} [f(\mathbf{w}, z)],$$

and the *empirical risk*

$$F_S(\mathbf{w}) \triangleq \frac{1}{n} \sum_{i=1}^n f(\mathbf{w}, z_i).$$

In practice, we cannot compute  $F_{\mathfrak{D}}(\mathbf{w})$  directly since the data distribution  $\mathfrak{D}$  is unknown. However, once the training set  $S$  is given, we have access to its estimation and can minimize the empirical risk  $F_S(\mathbf{w})$  instead, a process which is often referred to as *empirical risk minimization*. Let  $\mathbf{w}_{\mathcal{A}, S}$  be the output returned by minimizing the empirical risk  $F_S(\mathbf{w})$  with learning algorithm  $\mathcal{A}$ , and  $\mathbf{w}_{\mathfrak{D}}^*$  be one minimizer of the population risk  $F_{\mathfrak{D}}(\mathbf{w})$ , namely,  $\mathbf{w}_{\mathfrak{D}}^* \in \arg \min_{\mathbf{w}} F_{\mathfrak{D}}(\mathbf{w})$ . Since  $\mathbf{w}_{\mathcal{A}, S}$  in high probability will not be the same with  $\mathbf{w}_{\mathfrak{D}}^*$ , we are interested in how far  $\mathbf{w}_{\mathcal{A}, S}$  deviates from  $\mathbf{w}_{\mathfrak{D}}^*$  when evaluated on an unseen example  $z \sim \mathfrak{D}$ .

A natural measure to quantify this difference is the so-called *expected excess risk*,

$$\begin{aligned} \varepsilon_{exc} &\triangleq \mathbb{E} [F_{\mathfrak{D}}(\mathbf{w}_{\mathcal{A}, S}) - F_{\mathfrak{D}}(\mathbf{w}_{\mathfrak{D}}^*)] \\ &= \underbrace{\mathbb{E} [F_{\mathfrak{D}}(\mathbf{w}_{\mathcal{A}, S}) - F_S(\mathbf{w}_{\mathcal{A}, S})]}_{\varepsilon_{gen}} + \underbrace{\mathbb{E} [F_S(\mathbf{w}_{\mathcal{A}, S}) - F_S(\mathbf{w}_S^*)]}_{\varepsilon_{opt}} + \underbrace{\mathbb{E} [F_S(\mathbf{w}_S^*) - F_{\mathfrak{D}}(\mathbf{w}_{\mathfrak{D}}^*)]}_{\varepsilon_{approx}}, \end{aligned}$$

where  $\mathbf{w}_S^* \in \arg \min_{\mathbf{w}} F_S(\mathbf{w})$ . Since  $\mathbf{w}_{\mathfrak{D}}^*$  remains constant for the population risk  $F_{\mathfrak{D}}(\mathbf{w})$  which depends only on the data distribution and loss function, it follows that the *expected*

approximation error  $\varepsilon_{approx} = \mathbb{E}[F_S(\mathbf{w}_S^*) - F_{\mathcal{D}}(\mathbf{w}_{\mathcal{D}}^*)] = \mathbb{E}[F_S(\mathbf{w}_S^*) - F_S(\mathbf{w}_{\mathcal{D}}^*)] \leq 0$ . Therefore, it often suffices to obtain tight control of the *expected excess risk*  $\varepsilon_{exc}$  by bounding the *expected generalization error*<sup>2</sup>  $\varepsilon_{gen}$  and the *expected optimization error*  $\varepsilon_{opt}$ .

For learning algorithms based on iterative optimization,  $\varepsilon_{opt}$  in many cases can be analyzed via a convergence analysis (Bubeck et al., 2015). Meanwhile, to derive an upper bound over  $\varepsilon_{gen}$ , we can use the following theorem, which is due to Hardt et al. (2016), indicating that the generalization error could be bounded via the uniform stability (Bousquet and Elisseeff, 2002). Indeed, the uniform stability characterizes how sensitive the output of the learning algorithm  $\mathcal{A}$  is when a single example in the training set  $S$  is modified.

**Theorem 1 (Generalization error under  $\varepsilon$ -uniformly stability)** *Let  $S$  and  $S'$  denote two training sets i.i.d. sampled from the same data distribution  $\mathcal{D}$  such that  $S$  and  $S'$  differ in at most one example. A learning algorithm  $\mathcal{A}$  is  $\varepsilon$ -uniformly stable if and only if for all samples  $S$  and  $S'$ , the following inequality holds*

$$\sup_z \mathbb{E}|f(\mathbf{w}_{\mathcal{A},S}, z) - f(\mathbf{w}_{\mathcal{A},S'}, z)| \leq \varepsilon.$$

Furthermore, if  $\mathcal{A}$  is  $\varepsilon$ -uniformly stable, the expected generalization error  $\varepsilon_{gen}$  is upper bounded by  $\varepsilon$ , namely,

$$\mathbb{E}[F_{\mathcal{D}}(\mathbf{w}_{\mathcal{A},S}) - F_S(\mathbf{w}_{\mathcal{A},S})] \leq \varepsilon.$$

Before moving on, below we first introduce several definitions of the properties of the loss function  $f(\mathbf{w}, z)$ , which are quite common in the literature (Hardt et al., 2016; Bisla et al., 2022). To ease notation, we use  $f(\mathbf{w})$  interchangeably with  $f(\mathbf{w}, z)$  in the sequel as long as it is clear from the context that  $z$  is being held constant or can be understood from prior information.

**Definition 2 (Strong convexity)** *A function  $f(\mathbf{w}) : \mathbb{R}^d \mapsto \mathbb{R}_+$  is  $\mu$ -strongly convex, provided that*

$$\mu \mathbf{I} \preceq \nabla^2 f(\mathbf{w}), \quad \forall \mathbf{w} \in \mathbb{R}^d,$$

where  $\mathbf{I}$  represents the identity matrix.

**Definition 3 (Smoothness)** *A function  $f(\mathbf{w}) : \mathbb{R}^d \mapsto \mathbb{R}_+$  is  $L$ -smooth if for all  $\mathbf{v}, \mathbf{w} \in \mathbb{R}^d$  we have*

$$\|\nabla f(\mathbf{v}) - \nabla f(\mathbf{w})\|_2 \leq L \|\mathbf{v} - \mathbf{w}\|_2.$$

**Definition 4 (Lipschitz continuity)** *A function  $f(\mathbf{w}) : \mathbb{R}^d \mapsto \mathbb{R}_+$  is  $G$ -Lipschitz continuous if for all  $\mathbf{v}, \mathbf{w} \in \mathbb{R}^d$  we have*

$$|f(\mathbf{v}) - f(\mathbf{w})| \leq G \|\mathbf{v} - \mathbf{w}\|_2.$$

Given the above definitions, we can prove an auxiliary lemma that will be a cornerstone to show the main results.

---

2. It is worth noting that the difference between the test error and the training error in some literature is referred to as *generalization gap* and the test error alone goes by *generalization error*.



**Lemma 5** *A function  $f(\mathbf{w}) : \mathbb{R}^d \mapsto \mathbb{R}_+$  is  $\mu$ -strongly convex and  $L$ -smooth, for all  $\mathbf{w}, \mathbf{v} \in \mathbb{R}^d$ , we have*

$$\langle \nabla f(\mathbf{v}) - \nabla f(\mathbf{w}), \mathbf{v} - \mathbf{w} \rangle \geq \frac{\mu L}{\mu + L} \|\mathbf{v} - \mathbf{w}\|_2^2 + \frac{1}{\mu + L} \|\nabla f(\mathbf{v}) - \nabla f(\mathbf{w})\|_2^2.$$

**Proof** Consider the function  $\varphi(\mathbf{w}) \triangleq f(\mathbf{w}) - \frac{\mu}{2} \|\mathbf{w}\|_2^2$ , which is convex with  $(L - \mu)$ -smooth by appealing to the fact that  $f(\mathbf{w})$  is  $\mu$ -strongly convex and  $L$ -smooth. Therefore, it follows that

$$\langle \nabla \varphi(\mathbf{v}) - \nabla \varphi(\mathbf{w}), \mathbf{v} - \mathbf{w} \rangle \geq \frac{1}{L - \mu} \|\nabla \varphi(\mathbf{v}) - \nabla \varphi(\mathbf{w})\|_2^2.$$

On the other hand,

$$\langle \nabla \varphi(\mathbf{v}) - \nabla \varphi(\mathbf{w}), \mathbf{v} - \mathbf{w} \rangle = \langle \nabla f(\mathbf{v}) - \nabla f(\mathbf{w}), \mathbf{v} - \mathbf{w} \rangle - \mu \langle \mathbf{v} - \mathbf{w}, \mathbf{v} - \mathbf{w} \rangle.$$

Substituting the preceding inequality in, we have

$$\langle \nabla f(\mathbf{v}) - \nabla f(\mathbf{w}), \mathbf{v} - \mathbf{w} \rangle \geq \frac{\mu L}{\mu + L} \|\mathbf{v} - \mathbf{w}\|_2^2 + \frac{1}{\mu + L} \|\nabla f(\mathbf{v}) - \nabla f(\mathbf{w})\|_2^2,$$

thus concluding the proof. ■

## 4.2 Expected Excess Risk Analysis of SAM

In this section, we first investigate the stability of SAM and then its convergence property, together yielding an upper bound over the expected excess risk  $\varepsilon_{exc}$ . We restrict our attention to the strongly convex case so that we can compare against known results, particularly from Hardt et al. (2016).

### 4.2.1 STABILITY

Consider the parameter trajectories  $\mathbf{w}_1, \dots, \mathbf{w}_T$  and  $\mathbf{v}_1, \dots, \mathbf{v}_T$  induced by running SAM for  $T$  steps on sample  $S$  and  $S'$ , which differ from each other only by one single example. Suppose that the loss function  $f(\mathbf{w}, z)$  is  $G$ -Lipschitz with respect to the first argument, then it holds for all  $z \in Z$  that

$$|f(\mathbf{v}_T, z) - f(\mathbf{w}_T, z)| \leq G \|\mathbf{v}_T - \mathbf{w}_T\|_2. \quad (2)$$

Therefore, the remaining step in our setup is to upper bound  $\|\mathbf{v}_T - \mathbf{w}_T\|_2$ , which can be recursively controlled by the growth rate. Since  $S$  and  $S'$  differ in only one example, at every step  $t$ , the selected examples from  $S$  and  $S'$ , say  $z$  and  $z'$ , are either the same or not.

In the lemma below, we show that  $\|\mathbf{v}_t - \mathbf{w}_t\|_2$  is contracting when  $z$  and  $z'$  are the same. The technical difficulty mainly arises from how to lower bound  $\langle \mathbf{v}_t - \mathbf{w}_t, \nabla f(\mathbf{v}_t^{asc}) - \nabla f(\mathbf{w}_t^{asc}) \rangle$ , for which we require an additional assumption.

**Assumption 1** *Assume that at every step  $t$ , the loss function  $f(\mathbf{w})$  and  $f(\mathbf{v})$  are locally quadratic and their Hessians are the same, namely,  $\nabla^2 f(\mathbf{w})|_{\mathbf{w}_t} = \nabla^2 f(\mathbf{v})|_{\mathbf{v}_t} = \mathbf{H}_t$ , so that*

$$\nabla f(\mathbf{w}_t^{asc}) \triangleq \nabla f(\mathbf{w}_t + \xi_t^w \nabla f(\mathbf{w}_t)) = \nabla f(\mathbf{w}_t) + \xi_t^w \mathbf{H}_t \nabla f(\mathbf{w}_t),$$

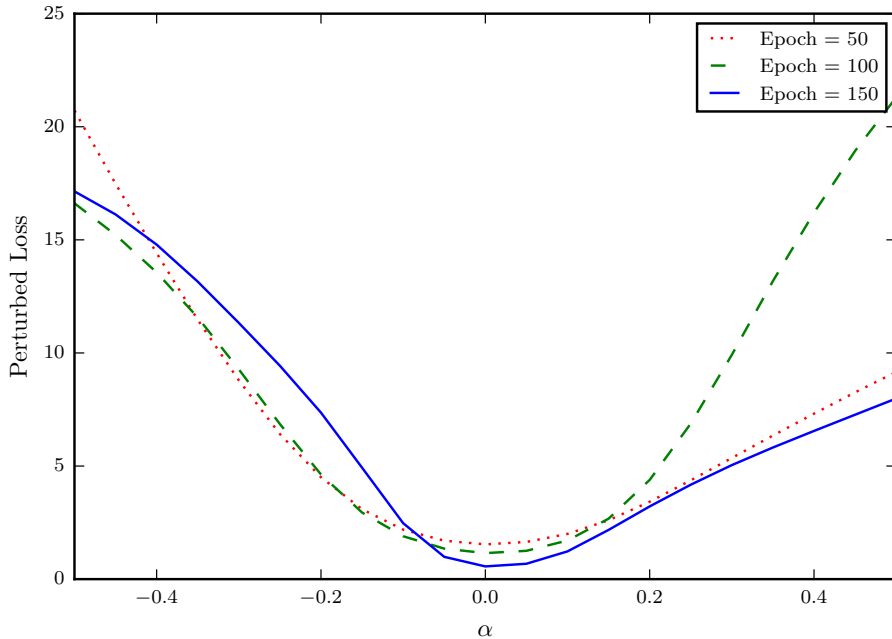


Figure 2: Evolution of perturbed loss landscape  $f(\mathbf{w} + \alpha \mathbf{e}_1)$ , where  $\mathbf{e}_1$  is the principal eigenvector of the Hessian  $\nabla^2 f(\mathbf{w})$  and  $\alpha \in [-0.5, 0.5]$ . The neural network, ResNet-20, is trained on CIFAR-100 up to 200 epochs using SGD optimizer with momentum acceleration, and the principal eigenvector is estimated using the PyHessian (Yao et al., 2020) library.

and

$$\nabla f(\mathbf{v}_t^{asc}) \triangleq \nabla f(\mathbf{v}_t + \xi_t^v \nabla f(\mathbf{v}_t)) = \nabla f(\mathbf{v}_t) + \xi_t^v \mathbf{H}_t \nabla f(\mathbf{v}_t),$$

where  $\xi_t^w = \rho / \|\nabla f(\mathbf{w}_t)\|_2$  and  $\xi_t^v = \rho / \|\nabla f(\mathbf{v}_t)\|_2$ . Furthermore, we require that  $\xi_t^w = \xi_t^v = \xi_t$  by adjusting the neighborhood size  $\rho$  at every step  $t$  and that there exists a constant  $C > 1$  such that  $\rho/G \leq \xi_t \leq C\rho/G$ .

This assumption follows Andriushchenko and Flammarion (2022) since it is difficult to analyze the growth rate of  $\|\mathbf{v}_t - \mathbf{w}_t\|_2$  directly as the update rule depends on the norm of  $\nabla f(\mathbf{w}_t)$  and  $\nabla f(\mathbf{v}_t)$ . It should be noted that the quadratic approximation is widely used to study the properties of SGD, for example, to analyze its diffusion behavior (Mandt et al., 2017) and learning dynamics (Wu et al., 2018). Although it does not necessarily hold in the early stages of training, however, as depicted in Figure 2, the quadratic approximation generally holds along the principal eigenvector of the Hessian during the entire training process. Despite the vanishing gradient  $\nabla f(\mathbf{w}_t)$ , the ratio  $\xi_t$  can still be controlled by decreasing the perturbation radius  $\rho$  proportionally with the gradient norm  $\|\nabla f(\mathbf{w}_t)\|_2$ . Under this assumption, our analysis can be greatly simplified.

**Lemma 6** Assume that the per-example loss function  $f(\mathbf{w}, z)$  satisfies Assumption 1 and is  $\mu$ -strongly convex,  $L$ -smooth and  $G$ -Lipschitz continuous with respect to the first argument  $\mathbf{w}$ . Suppose that at step  $t$ , the examples selected by SAM are the same in  $S$  and  $S'$  and the corresponding parameter update rule is denoted by  $\mathbf{w}_{t+1} = \mathbf{w}_t - \eta \nabla f(\mathbf{w}_t^{asc}, z)$  and  $\mathbf{v}_{t+1} =$

$\mathbf{v}_t - \eta \nabla f(\mathbf{v}_t^{asc}, z)$ , respectively. Then, if the learning rate satisfies  $\eta \leq 2(1 + \mu\rho/G)/(\mu + L)(1 + CL\rho/G)^2$ , it follows that

$$\|\mathbf{v}_{t+1} - \mathbf{w}_{t+1}\|_2 \leq \left(1 - \left(1 + \mu \frac{\rho}{G}\right) \frac{\eta\mu L}{\mu + L}\right) \|\mathbf{v}_t - \mathbf{w}_t\|_2.$$

**Proof** Since the loss function  $f(\mathbf{w})$  is  $\mu$ -strongly convex and  $L$ -smooth, it follows that the eigenvalues of the Hessian  $\mathbf{H}_t$  satisfy the inequality below

$$\mu \leq \sigma_{\min}(\mathbf{H}_t) \leq \sigma_{\max}(\mathbf{H}_t) \leq L.$$

Recall the parameter update rule of SAM, we have

$$\begin{aligned} \|\mathbf{v}_{t+1} - \mathbf{w}_{t+1}\|_2^2 &= \|\mathbf{v}_t - \eta \nabla f(\mathbf{v}_t^{asc}) - (\mathbf{w}_t - \eta \nabla f(\mathbf{w}_t^{asc}))\|_2^2 \\ &= \|\mathbf{v}_t - \mathbf{w}_t\|_2^2 - 2\eta \langle \mathbf{v}_t - \mathbf{w}_t, \nabla f(\mathbf{v}_t^{asc}) - \nabla f(\mathbf{w}_t^{asc}) \rangle + \eta^2 \|\nabla f(\mathbf{v}_t^{asc}) - \nabla f(\mathbf{w}_t^{asc})\|_2^2 \\ &= \|\mathbf{v}_t - \mathbf{w}_t\|_2^2 - 2\eta \langle \mathbf{v}_t - \mathbf{w}_t, (\mathbf{I} + \xi_t \mathbf{H}_t) (\nabla f(\mathbf{v}_t) - \nabla f(\mathbf{w}_t)) \rangle \\ &\quad + \eta^2 \|(\mathbf{I} + \xi_t \mathbf{H}_t) (\nabla f(\mathbf{v}_t) - \nabla f(\mathbf{w}_t))\|_2^2 \\ &\leq \|\mathbf{v}_t - \mathbf{w}_t\|_2^2 - 2\eta (1 + \xi_t \sigma_{\min}(\mathbf{H}_t)) \langle \mathbf{v}_t - \mathbf{w}_t, \nabla f(\mathbf{v}_t) - \nabla f(\mathbf{w}_t) \rangle \\ &\quad + \eta^2 (1 + \xi_t \sigma_{\max}(\mathbf{H}_t))^2 \|\nabla f(\mathbf{v}_t) - \nabla f(\mathbf{w}_t)\|_2^2 \\ &\stackrel{\textcircled{1}}{\leq} \left(1 - 2(1 + \xi_t \sigma_{\min}(\mathbf{H}_t)) \frac{\eta\mu L}{\mu + L}\right) \|\mathbf{v}_t - \mathbf{w}_t\|_2^2 \\ &\quad + \left(\eta^2 (1 + \xi_t \sigma_{\max}(\mathbf{H}_t))^2 - \frac{2\eta(1 + \xi_t \sigma_{\min}(\mathbf{H}_t))}{\mu + L}\right) \|\nabla f(\mathbf{v}_t) - \nabla f(\mathbf{w}_t)\|_2^2 \\ &\stackrel{\textcircled{2}}{\leq} \left(1 - 2(1 + \xi_t \sigma_{\min}(\mathbf{H}_t)) \frac{\eta\mu L}{\mu + L}\right) \|\mathbf{v}_t - \mathbf{w}_t\|_2^2 \\ &\stackrel{\textcircled{3}}{\leq} \left(1 - 2\left(1 + \frac{\rho}{G}\mu\right) \frac{\eta\mu L}{\mu + L}\right) \|\mathbf{v}_t - \mathbf{w}_t\|_2^2, \end{aligned}$$

where  $\textcircled{1}$  is due to the coercivity of the loss function (Lemma 5) that

$$\langle \nabla f(\mathbf{v}) - \nabla f(\mathbf{w}), \mathbf{v} - \mathbf{w} \rangle \geq \frac{\mu L}{\mu + L} \|\mathbf{v} - \mathbf{w}\|_2^2 + \frac{1}{\mu + L} \|\nabla f(\mathbf{v}) - \nabla f(\mathbf{w})\|_2^2.$$

Moreover,  $\textcircled{2}$  holds since the second term of  $\textcircled{1}$  is smaller than zero provided that the learning rate  $\eta$  satisfies the given condition and  $\textcircled{3}$  follows by appealing to the fact that  $\xi_t$  is lower bounded by  $\rho/G$ . Consequently, we have

$$\|\mathbf{v}_{t+1} - \mathbf{w}_{t+1}\|_2 \leq \left(1 - 2\left(1 + \frac{\rho}{G}\mu\right) \frac{\eta\mu L}{\mu + L}\right)^{1/2} \|\mathbf{v}_t - \mathbf{w}_t\|_2 \leq \left(1 - \left(1 + \frac{\rho}{G}\mu\right) \frac{\eta\mu L}{\mu + L}\right) \|\mathbf{v}_t - \mathbf{w}_t\|_2,$$

where the last inequality is due to the fact that  $\sqrt{1-x} \leq 1-x/2$  holds for all  $x \in [0, 1]$ .  $\blacksquare$

On the other hand, with probability  $1/n$ , the examples selected by SAM, say  $z$  and  $z'$ , are different in both  $S$  and  $S'$ . In this case, we can simply bound the growth in  $\|\mathbf{v}_t - \mathbf{w}_t\|_2$  by the norms of  $\nabla f(\mathbf{v}, z)$  and  $\nabla f(\mathbf{w}, z')$  as follows.

**Lemma 7** Assume the same settings as in Lemma 6. For the  $t$ -th iteration, suppose that the examples selected by SAM are different in  $S$  and  $S'$  and that  $\mathbf{w}_{t+1} = \mathbf{w}_t - \eta \nabla f(\mathbf{w}_t^{asc}, z)$  and  $\mathbf{v}_{t+1} = \mathbf{v}_t - \eta \nabla f(\mathbf{v}_t^{asc}, z')$ , where  $\eta \leq 2(1 + \mu\rho/G)/(\mu + L)(1 + CL\rho/G)^2$ . Consequently, we have

$$\|\mathbf{v}_{t+1} - \mathbf{w}_{t+1}\|_2 \leq \left(1 - \left(1 + \mu \frac{\rho}{G}\right) \frac{\eta\mu L}{\mu + L}\right) \|\mathbf{v}_t - \mathbf{w}_t\|_2 + 2\eta G.$$

**Proof** The proof is straightforward. It follows immediately

$$\begin{aligned} \|\mathbf{v}_{t+1} - \mathbf{w}_{t+1}\|_2 &= \|\mathbf{v}_t - \eta \nabla f(\mathbf{v}_t^{asc}, z') - (\mathbf{w}_t - \eta \nabla f(\mathbf{w}_t^{asc}, z')) - \eta (\nabla f(\mathbf{w}_t^{asc}, z') - \nabla f(\mathbf{w}_t^{asc}, z))\|_2 \\ &\leq \|\mathbf{v}_t - \eta \nabla f(\mathbf{v}_t^{asc}, z') - (\mathbf{w}_t - \eta \nabla f(\mathbf{w}_t^{asc}, z'))\|_2 + \eta \|\nabla f(\mathbf{w}_t^{asc}, z') - \nabla f(\mathbf{w}_t^{asc}, z)\|_2 \\ &\leq \left(1 - \left(1 + \mu \frac{\rho}{G}\right) \frac{\eta\mu L}{\mu + L}\right) \|\mathbf{v}_t - \mathbf{w}_t\|_2 + 2\eta G, \end{aligned}$$

where the last inequality comes from Lemma 6. ■

With the above two lemmas, we are now ready to give an upper bound over the expected generalization error of SAM.

**Theorem 8** Assume the loss function  $f(\mathbf{w}; z)$  is  $\mu$ -strongly convex and  $L$ -smooth for all  $z \in Z$ . Suppose we run the SAM iteration with constant learning rate  $\eta \leq 2(1 + \mu\rho/G)/(\mu + L)(1 + CL\rho/G)^2$  for  $T$  steps. Then, SAM satisfies uniform stability with

$$\varepsilon_{\text{gen}} \leq \frac{2G^2(\mu + L)}{n\mu L(1 + \mu\rho/G)}.$$

**Proof** Define  $\delta_t \triangleq \|\mathbf{w}_t - \mathbf{v}_t\|_2$  to denote the Euclidean distance between  $\mathbf{w}_t$  and  $\mathbf{v}_t$  as training progresses. Observe that at any step  $t \leq T$ , with a probability  $1 - 1/n$ , the selected examples from  $S$  and  $S'$  are the same. In contrast, with a probability of  $1/n$ , the selected examples are different. This is because  $S$  and  $S'$  only differ by one example. Therefore, from Lemmas 6 and 7, we conclude that

$$\begin{aligned} \mathbb{E}[\delta_t] &\leq \left(1 - \frac{1}{n}\right) \left(1 - \left(1 + \mu \frac{\rho}{G}\right) \frac{\eta\mu L}{\mu + L}\right) \mathbb{E}[\delta_{t-1}] + \frac{1}{n} \left(1 - \left(1 + \mu \frac{\rho}{G}\right) \frac{\eta\mu L}{\mu + L}\right) \mathbb{E}[\delta_{t-1}] + \frac{2\eta G}{n} \\ &= \left(1 - \left(1 + \mu \frac{\rho}{G}\right) \frac{\eta\mu L}{\mu + L}\right) \mathbb{E}[\delta_{t-1}] + \frac{2\eta G}{n}. \end{aligned}$$

Unraveling the above recursion yields

$$\mathbb{E}[\delta_T] \leq \frac{2\eta G}{n} \sum_{t=0}^{T-1} \left(1 - \left(1 + \mu \frac{\rho}{G}\right) \frac{\eta\mu L}{\mu + L}\right)^t \leq \frac{2G(\mu + L)}{n\mu L(1 + \mu\rho/G)}.$$

Plugging this inequality into (2), we obtain

$$\mathbb{E}|f(\mathbf{w}_T; z) - f(\mathbf{v}_T; z)| \leq \frac{2G^2(\mu + L)}{n\mu L(1 + \mu\rho/G)}.$$

The proof is completed. ■

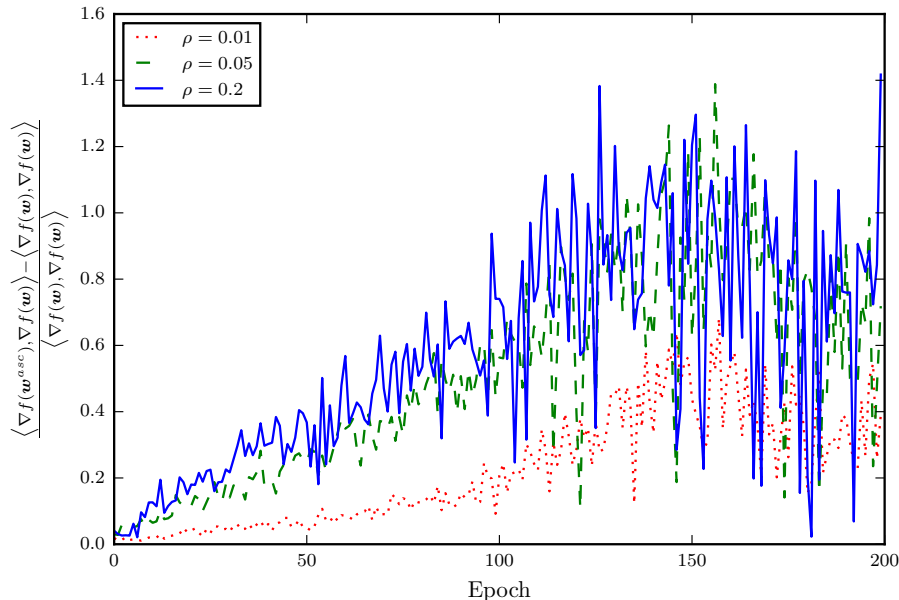


Figure 3: Well-alignment between the surrogate gradient  $\nabla f(\mathbf{w}^{asc})$  and the exact gradient  $\nabla f(\mathbf{w})$  when both evaluated on the same mini-batch per training step. The positiveness of  $y$ -axis suggests that the cross-product between  $\nabla f(\mathbf{w}^{asc})$  and  $\nabla f(\mathbf{w})$  is larger than the norm of  $\nabla f(\mathbf{w})$  during the entire training stage.

**Remark 9** In the same strongly convex setting, *Hardt et al. (2016)* showed that SGD can attain an upper bound  $\varepsilon_{gen} \leq \frac{2G^2(\mu+L)}{n\mu L}$  with a prerequisite  $\eta \leq \frac{2}{\mu+L}$ . This theorem, however, suggests that SAM can generalize better than SGD because of the additional term  $1 + \mu\rho/G$  in the denominator, though the conclusion only holds for a much smaller learning rate  $\eta \leq \frac{2}{\mu+L} \frac{1+\mu\rho/G}{(1+CL\rho/G)^2}$ .

#### 4.2.2 CONVERGENCE

From the perspective of convergence, we can further prove that SAM converges to a smaller noise ball if the learning rate  $\eta$  is fixed.

**Theorem 10** Suppose the loss function  $f(\mathbf{w}, z)$  is  $\mu$ -strongly convex,  $L$ -smooth, and  $G$ -Lipschitz continuous with respect to the first argument  $\mathbf{w}$ . Consider the sequence  $\mathbf{w}_1, \dots, \mathbf{w}_T$  generated by running SAM with a constant learning rate  $\eta$ . Let  $\mathbf{w}^* \in \arg \inf_{\mathbf{w}} f(\mathbf{w})$ , it follows that for any  $1 \leq t \leq T$ ,

$$\mathbb{E}[f(\mathbf{w}_T) - f(\mathbf{w}^*)] \leq (1 - 2\mu\eta(1 + \mu\rho/G))^T \mathbb{E}[f(\mathbf{w}_0) - f(\mathbf{w}^*)] + \frac{\eta G^2 L}{4\mu(1 + \mu\rho/G)}.$$

**Proof** Since  $f(\mathbf{w})$  is  $L$ -smooth and  $G$ -Lipschitz, from Taylor's theorem, there exists a  $\hat{\mathbf{w}}_t$  such that

$$\begin{aligned}
f(\mathbf{w}_{t+1}) &= f(\mathbf{w}_t - \eta \nabla f(\mathbf{w}_t^{asc})) \\
&= f(\mathbf{w}_t) - \eta \nabla f(\mathbf{w}_t^{asc})^T \nabla f(\mathbf{w}_t) + \frac{1}{2} \eta \nabla f(\mathbf{w}_t^{asc})^T \nabla^2 f(\hat{\mathbf{w}}_t) (\eta \nabla f(\mathbf{w}_t^{asc})) \\
&\leq f(\mathbf{w}_t) - \eta \nabla f(\mathbf{w}_t^{asc})^T \nabla f(\mathbf{w}_t) + \frac{\eta^2 L}{2} \|\nabla f(\mathbf{w}_t^{asc})\|_2^2 \\
&\leq f(\mathbf{w}_t) - \eta \nabla f(\mathbf{w}_t^{asc})^T \nabla f(\mathbf{w}_t) + \frac{\eta^2 L G^2}{2}.
\end{aligned}$$

On the other hand,

$$\begin{aligned}
\nabla f(\mathbf{w}_t^{asc})^T \nabla f(\mathbf{w}_t) &= \nabla f(\mathbf{w}_t + \xi_t \nabla f(\mathbf{w}_t))^T \nabla f(\mathbf{w}_t) \\
&\stackrel{\textcircled{1}}{\geq} (1 + \mu \xi_t) \|\nabla f(\mathbf{w}_t)\|_2^2 \\
&\stackrel{\textcircled{2}}{\geq} 2\mu(1 + \mu \xi_t)(f(\mathbf{w}_t) - f(\mathbf{w}^*)) \\
&\geq 2\mu(1 + \mu \rho/G)(f(\mathbf{w}_t) - f(\mathbf{w}^*)),
\end{aligned}$$

where  $\textcircled{1}$  holds because  $\nabla f(\mathbf{w})$  and  $\nabla f(\mathbf{w}^{asc})$  are both evaluated on the same mini-batch and we have

$$\begin{aligned}
\langle \nabla f(\mathbf{w}_t + \xi_t \nabla f(\mathbf{w}_t)), \nabla f(\mathbf{w}_t) \rangle &= \langle \nabla f(\mathbf{w}_t + \xi_t \nabla f(\mathbf{w}_t)) - \nabla f(\mathbf{w}_t), \nabla f(\mathbf{w}_t) \rangle + \|\nabla f(\mathbf{w}_t)\|_2^2 \\
&= \frac{1}{\xi_t} \langle \nabla f(\mathbf{w}_t^{asc}) - \nabla f(\mathbf{w}_t), \mathbf{w}_t^{asc} - \mathbf{w}_t \rangle + \|\nabla f(\mathbf{w}_t)\|_2^2 \\
&\geq \frac{1}{\xi_t} \mu \|\mathbf{w}_t^{asc} - \mathbf{w}_t\|_2^2 + \|\nabla f(\mathbf{w}_t)\|_2^2 \\
&= (1 + \mu \xi_t) \|\nabla f(\mathbf{w}_t)\|_2^2.
\end{aligned}$$

The inequality that  $\langle \nabla f(\mathbf{w}_t^{asc}), \nabla f(\mathbf{w}_t) \rangle$  is larger than  $\langle \nabla f(\mathbf{w}_t), \nabla f(\mathbf{w}_t) \rangle$  can be numerically verified, see Figure 3 for an illustration. And  $\textcircled{2}$  is due to Polyak-Łojasiewicz condition as a result of being  $\mu$ -strongly convex. Subtracting  $f(\mathbf{w}^*)$  from both sides and taking expectations, we obtain

$$\mathbb{E}[f(\mathbf{w}_{t+1}) - f(\mathbf{w}^*)] \leq (1 - 2\mu\eta(1 + \mu\rho/G))\mathbb{E}[f(\mathbf{w}_t) - f(\mathbf{w}^*)] + \frac{\eta^2 G^2 L}{2}.$$

Recursively applying the above inequality and summing up the geometric series yields

$$\mathbb{E}[f(\mathbf{w}_T) - f(\mathbf{w}^*)] \leq (1 - 2\mu\eta(1 + \mu\rho/G))^T \mathbb{E}[f(\mathbf{w}_0) - f(\mathbf{w}^*)] + \frac{\eta G^2 L}{4\mu(1 + \mu\rho/G)},$$

thus concluding the proof. ■

Combining the previous results, we are able to present an upper bound over the expected excess risk of the SAM algorithm.

**Theorem 11** *Under assumptions and parameter settings in Theorems 8 and 10, the expected excess risk  $\varepsilon_{exc}$  of the output  $\mathbf{w}_T$  obeys  $\varepsilon_{exc} \leq \varepsilon_{gen} + \varepsilon_{opt}$ , where  $\varepsilon_{opt}$  and  $\varepsilon_{gen}$  are given by Theorems 8 and 10, respectively. Furthermore, as  $T$  grows to infinity, we have*

$$\varepsilon_{exc} \leq \frac{2G^2(\mu + L)}{n\mu L(1 + \mu\rho/G)} + \frac{\eta G^2 L}{4\mu(1 + \mu\rho/G)}.$$

**Proof** This result is given by the fact that  $(1 - 2\mu\eta(1 + \mu\rho/G))^T$  converges to zero as  $T \rightarrow \infty$ . ■

**Remark 12** *We note that this bound resembles that of SGD, except with a multiplier  $\frac{1}{1+\mu\rho/G}$ . Therefore, in a restricted regime of learning rate, we can observe that SAM achieves a tighter bound over the expected excess risk than SGD and that the generalization performance of SAM increases with the perturbation radius  $\rho$ , a phenomenon which is quite common in many applications. However, it should also be remembered that the choice of  $\rho$  also controls the trainability of the deep neural networks since a too large value of  $\rho$  could result in gradient explosion.*

### 4.3 Expected Excess Risk Analysis of StableSAM

Now we continue to investigate the stability of sharpness-aware training when the renormalization strategy is applied. Compared to SAM, by imposing a stronger condition on the smallest eigenvalue of the Hessian, we demonstrate that StableSAM allows for a relatively larger learning rate without performance deterioration. We also discuss when StableSAM can consistently achieve a better performance than SAM.

#### 4.3.1 STABILITY

Let  $\gamma_t$  denote the renormalization factor  $\|\nabla f(\mathbf{w}_t)\|_2 / \|\nabla f(\mathbf{w}_t^{asc})\|_2$  in Algorithm 1. To proceed, we require two assumptions as follows.

**Assumption 2** *Suppose that there exist two constants  $\gamma_0$  and  $\gamma_1$  so that  $\gamma_t$  is bounded for all  $1 \leq t \leq T$*

$$0 < \gamma_0 \leq \gamma_t \leq \gamma_1 < 1.$$

**Assumption 3** *Assume that the smallest eigenvalue of the Hessian  $\mathbf{H}_t$  is bounded below for all  $1 \leq t \leq T$*

$$\sigma_{\min}(\mathbf{H}_t) \geq \frac{G}{\rho} \frac{1 - \gamma_0}{\gamma_0} + \frac{\mu}{\gamma_0}.$$

The first assumption can be easily checked (see Figure 1). The second assumption is valid since minimizing the ascent-direction sharpness is equivalent to regularizing the smallest non-zero eigenvalue of the Hessian (Wen et al., 2022) and the renormalization step indeed reduces the strength of the regularization and thus corresponds to a larger smallest eigenvalue. Under these assumptions, we can derive the same growth rate of  $\|\mathbf{v}_t - \mathbf{w}_t\|_2$  as Lemma 6.

**Lemma 13** *Let Assumptions 1, 2 and 3 hold and assume that the per-example loss function  $f(\mathbf{w}, z)$  is  $\mu$ -strongly convex,  $L$ -smooth and  $G$ -Lipschitz continuous with respect to the first argument  $\mathbf{w}$ . Suppose that at step  $t$ , the examples selected by StableSAM are the same in  $S$  and  $S'$  and the corresponding parameter update rule is denoted by  $\mathbf{w}_{t+1} = \mathbf{w}_t - \eta\gamma_t\nabla f(\mathbf{w}_t^{asc}, z)$  and  $\mathbf{v}_{t+1} = \mathbf{v}_t - \eta\gamma_t\nabla f(\mathbf{v}_t^{asc}, z)$ , respectively. Then, if the learning rate satisfies  $\eta \leq 2(1 + \mu\rho/G)/\gamma_1(\mu + L)(1 + CL\rho/G)^2$ , it follows that*

$$\|\mathbf{v}_{t+1} - \mathbf{w}_{t+1}\|_2 \leq \left(1 - \left(1 + \mu\frac{\rho}{G}\right)\frac{\eta\mu L}{\mu + L}\right)\|\mathbf{v}_t - \mathbf{w}_t\|_2.$$

**Proof** The proof is the same with Lemma 6.  $\blacksquare$

On the other hand, when the examples selected from  $S$  and  $S'$  are different, we can obtain a similar result as Lemma 7.

**Lemma 14** *Assume the same settings as in Lemma 13. For the  $t$ -th iteration, suppose that the examples selected by StableSAM are different in  $S$  and  $S'$  and that  $\mathbf{w}_{t+1} = \mathbf{w}_t - \eta\gamma_t\nabla f(\mathbf{w}_t^{asc}, z)$  and  $\mathbf{v}_{t+1} = \mathbf{v}_t - \eta\gamma_t\nabla f(\mathbf{v}_t^{asc}, z')$ . Consequently, we obtain*

$$\|\mathbf{v}_{t+1} - \mathbf{w}_{t+1}\|_2 \leq \left(1 - \left(1 + \mu\frac{\rho}{G}\right)\frac{\eta\mu L}{\mu + L}\right)\|\mathbf{v}_t - \mathbf{w}_t\|_2 + 2\eta\gamma_1 G.$$

**Proof** The proof is straightforward. It follows immediately from

$$\begin{aligned} \|\mathbf{v}_{t+1} - \mathbf{w}_{t+1}\|_2 &= \|\mathbf{v}_t - \eta\gamma_t\nabla f(\mathbf{v}_t^{asc}, z') - (\mathbf{w}_t - \eta\gamma_t\nabla f(\mathbf{v}_t^{asc}, z')) - \eta\gamma_t(\nabla f(\mathbf{v}_t^{asc}, z') - \nabla f(\mathbf{w}_t^{asc}, z))\|_2 \\ &\leq \|\mathbf{v}_t - \eta\gamma_t\nabla f(\mathbf{v}_t^{asc}, z') - (\mathbf{w}_t - \eta\gamma_t\nabla f(\mathbf{v}_t^{asc}, z'))\|_2 + \eta\gamma_t\|\nabla f(\mathbf{v}_t^{asc}, z') - \nabla f(\mathbf{w}_t^{asc}, z)\|_2 \\ &\leq \left(1 - \left(1 + \mu\frac{\rho}{G}\right)\frac{\eta\mu L}{\mu + L}\right)\|\mathbf{v}_t - \mathbf{w}_t\|_2 + 2\eta\gamma_1 G, \end{aligned}$$

thus concluding the proof.  $\blacksquare$

With the above two lemmas, we show that StableSAM consistently performs better than SAM in terms of the generalization error.

**Theorem 15** *Under assumptions and parameter settings in Lemmas 13 and 14. Suppose we run the StableSAM iteration with constant learning rate  $\eta \leq 2(1 + \mu\rho/G)/\gamma_1(\mu + L)(1 + CL\rho/G)^2$  for  $T$  steps. Then, StableSAM satisfies uniform stability with*

$$\varepsilon_{\text{gen}} \leq \frac{2\gamma_1 G^2(\mu + L)}{n\mu L(1 + \mu\rho/G)}.$$

**Proof** Define  $\delta_t \triangleq \|\mathbf{w}_t - \mathbf{v}_t\|_2$  to denote the Euclidean distance between  $\mathbf{w}_t$  and  $\mathbf{v}_t$  as training continues. Observe that at any step  $t \leq T$ , with a probability  $1 - 1/n$ , the selected examples from  $S$  and  $S'$  are the same. In contrast, with a probability of  $1/n$ , the selected examples are different. This is because  $S$  and  $S'$  only differ by one example. Therefore, from Lemmas 13 and 14, we conclude that

$$\begin{aligned} \mathbb{E}[\delta_t] &\leq \left(1 - \frac{1}{n}\right)\left(1 - \left(1 + \frac{\rho}{G}\mu\right)\frac{\eta\mu L}{\mu + L}\right)\mathbb{E}[\delta_{t-1}] + \frac{1}{n}\left(1 - \left(1 + \frac{\rho}{G}\mu\right)\frac{\eta\mu L}{\mu + L}\right)\mathbb{E}[\delta_{t-1}] + \frac{2\eta\gamma_1 G}{n} \\ &= \left(1 - \left(1 + \frac{\rho}{G}\mu\right)\frac{\eta\mu L}{\mu + L}\right)\mathbb{E}[\delta_{t-1}] + \frac{2\eta\gamma_1 G}{n}. \end{aligned}$$



Unraveling the above recursion yields

$$\mathbb{E}[\delta_T] \leq \frac{2\eta\gamma_1 G}{n} \sum_{t=0}^T \left( 1 - \left( 1 + \frac{\rho}{G}\mu \right) \frac{\eta\mu L}{\mu + L} \right)^t \leq \frac{2\gamma_1 G(\mu + L)}{n\mu L(1 + \mu\rho/G)}.$$

Plugging this inequality into (2), we obtain

$$\mathbb{E}|f(\mathbf{w}_T; z) - f(\mathbf{v}_T; z)| \leq \frac{2\gamma_1 G^2(\mu + L)}{n\mu L(1 + \mu\rho/G)}.$$

The proof is completed. ■

**Remark 16** *Compared to SAM, this theorem indicates that the upper bound over expected generalization error can be further reduced from  $\frac{2G^2(\mu+L)}{n\mu L(1+\mu\rho/G)}$  to  $\frac{2\gamma_1 G^2(\mu+L)}{n\mu L(1+\mu\rho/G)}$ , even with a relatively larger learning rate. Surprisingly, this reduction exhibits a negative correlation with  $\gamma_1$ , which reflects the structure of the loss landscape at the current location. Namely, the renormalization strategy is more effective when  $\gamma_1$  is relatively small and the corresponding loss landscape is rugged.*

#### 4.3.2 CONVERGENCE

Similar to Theorem 10, we show that StableSAM also converges to a noise ball when the learning rate  $\eta$  is fixed.

**Theorem 17** *Let Assumption 2 hold and suppose the loss function  $f(\mathbf{w}, z)$  is  $\mu$ -strongly convex,  $L$ -smooth, and  $G$ -Lipschitz continuous with respect to the first argument  $\mathbf{w}$ . Consider the sequence  $\mathbf{w}_1, \dots, \mathbf{w}_T$  generated by running StableSAM with a constant learning rate  $\eta$  for  $T$  steps. Let  $\mathbf{w}^* \in \arg \inf_{\mathbf{w}} f(\mathbf{w})$ , it follows that for any  $1 \leq t \leq T$ ,*

$$\mathbb{E}[f(\mathbf{w}_T) - f(\mathbf{w}^*)] \leq (1 - 2\mu\gamma_0\eta(1 + \mu\rho/G))^T \mathbb{E}[f(\mathbf{w}_0) - f(\mathbf{w}^*)] + \frac{\eta\gamma_1^2 G^2 L}{4\mu\gamma_0(1 + \mu\rho/G)}.$$

**Proof** Since  $f(\mathbf{w})$  is  $L$ -smooth and  $G$ -Lipschitz, it follows that

$$\begin{aligned} f(\mathbf{w}_{t+1}) &= f(\mathbf{w}_t - \eta\gamma_t \nabla f(\mathbf{w}_t^{asc})) \\ &= f(\mathbf{w}_t) - \eta\gamma_t \nabla f(\mathbf{w}_t^{asc})^T \nabla f(\mathbf{w}_t) + \frac{1}{2} (\eta\gamma_t \nabla f(\mathbf{w}_t^{asc}))^T \nabla^2 f(\hat{\mathbf{w}}_t) (\eta\gamma_t \nabla f(\mathbf{w}_t^{asc})) \\ &\leq f(\mathbf{w}_t) - \eta\gamma_t \nabla f(\mathbf{w}_t^{asc})^T \nabla f(\mathbf{w}_t) + \frac{\eta^2 \gamma_t^2 L}{2} \|\nabla f(\mathbf{w}_t^{asc})\|_2^2 \\ &\leq f(\mathbf{w}_t) - \eta\gamma_t \nabla f(\mathbf{w}_t^{asc})^T \nabla f(\mathbf{w}_t) + \frac{\eta^2 \gamma_t^2 L G^2}{2}. \end{aligned}$$

On the other hand, with a similar argument as in Theorem 10, we have

$$\nabla f(\mathbf{w}_t^{asc})^T \nabla f(\mathbf{w}_t) \geq 2\mu(1 + \mu\rho/G)(f(\mathbf{w}_t) - f(\mathbf{w}^*)).$$

Hence, subtracting  $f(\mathbf{w}^*)$  from both sides and taking expectations, we obtain

$$\begin{aligned}\mathbb{E}[f(\mathbf{w}_{t+1}) - f(\mathbf{w}^*)] &\leq (1 - 2\mu\eta\gamma_t(1 + \mu\rho/G))\mathbb{E}[f(\mathbf{w}_t) - f(\mathbf{w}^*)] + \frac{\eta^2\gamma_t^2G^2L}{2} \\ &\leq (1 - 2\mu\eta\gamma_0(1 + \mu\rho/G))\mathbb{E}[f(\mathbf{w}_t) - f(\mathbf{w}^*)] + \frac{\eta^2\gamma_1^2G^2L}{2}.\end{aligned}$$

Applying the recurrence relation, yields

$$\mathbb{E}[f(\mathbf{w}_T) - f(\mathbf{w}^*)] \leq (1 - 2\mu\eta\gamma_0(1 + \mu\rho/G))^T \mathbb{E}[f(\mathbf{w}_0) - f(\mathbf{w}^*)] + \frac{\eta\gamma_1^2G^2L}{4\gamma_0\mu(1 + \mu\rho/G)},$$

thus concluding the proof.  $\blacksquare$

Combining these results, we can present an upper bound over the expected excess risk of the StableSAM algorithm as follows.

**Theorem 18** *Under assumptions and parameter settings in Theorems 15 and 17, the expected excess risk  $\varepsilon_{exc}$  of the output  $\mathbf{w}_T$  obeys  $\varepsilon_{exc} \leq \varepsilon_{opt} + \varepsilon_{gen}$ , where  $\varepsilon_{opt}$  and  $\varepsilon_{gen}$  are given by Theorems 15 and 17, respectively. Furthermore, as  $T$  tends to infinity, we have*

$$\varepsilon_{exc} \leq \frac{2\gamma_1G^2(\mu + L)}{n\mu L(1 + \mu\rho/G)} + \frac{\eta\gamma_1^2G^2L}{4\gamma_0\mu(1 + \mu\rho/G)}.$$

**Proof** This result is given by the fact that  $(1 - 2\mu\eta\gamma_0(1 + \mu\rho/G))^T$  converges to zero as  $T \rightarrow \infty$ .  $\blacksquare$

**Remark 19** *Theoretically, when  $\gamma_0 = \gamma_1$ , we can infer from the above theorem that StableSAM consistently performs better than SAM. However, this is an unrealistic condition in practice. Indeed, if we adjust the renormalization factor at every step so that  $\gamma_1^2 \leq \gamma_0$ , StableSAM still can attain a lower expected excess risk bound than SAM. This can be easily implemented, for example, by constraining that  $\gamma_t = \min(\max(\|\nabla f(\mathbf{w}_t)\|_2 / \|\nabla f(\mathbf{w}_t^{asc})\|_2, \gamma_0), \sqrt{\gamma_0})$  for any predefined  $\gamma_0 \in (0, 1)$ . However, such an operation requires very careful tuning as an inappropriate initialization of  $\gamma_0$  will break up the Assumption 3 and turn over the conclusion.*

## 5. Experiments

In this section, we present the empirical results on a range of tasks. Starting with a toy example, we show that StableSAM can greatly ameliorate the issue of training instability in sharpness-aware training. We further investigate this issue from the perspective of uniform stability with realistic data sets. To demonstrate that the increased stability does not come at the cost of performance degradation, we also evaluate it on tasks such as training deep classifiers from scratch and learning with noisy labels. The results suggest that StableSAM can achieve comparable or even superior performance compared to SAM.

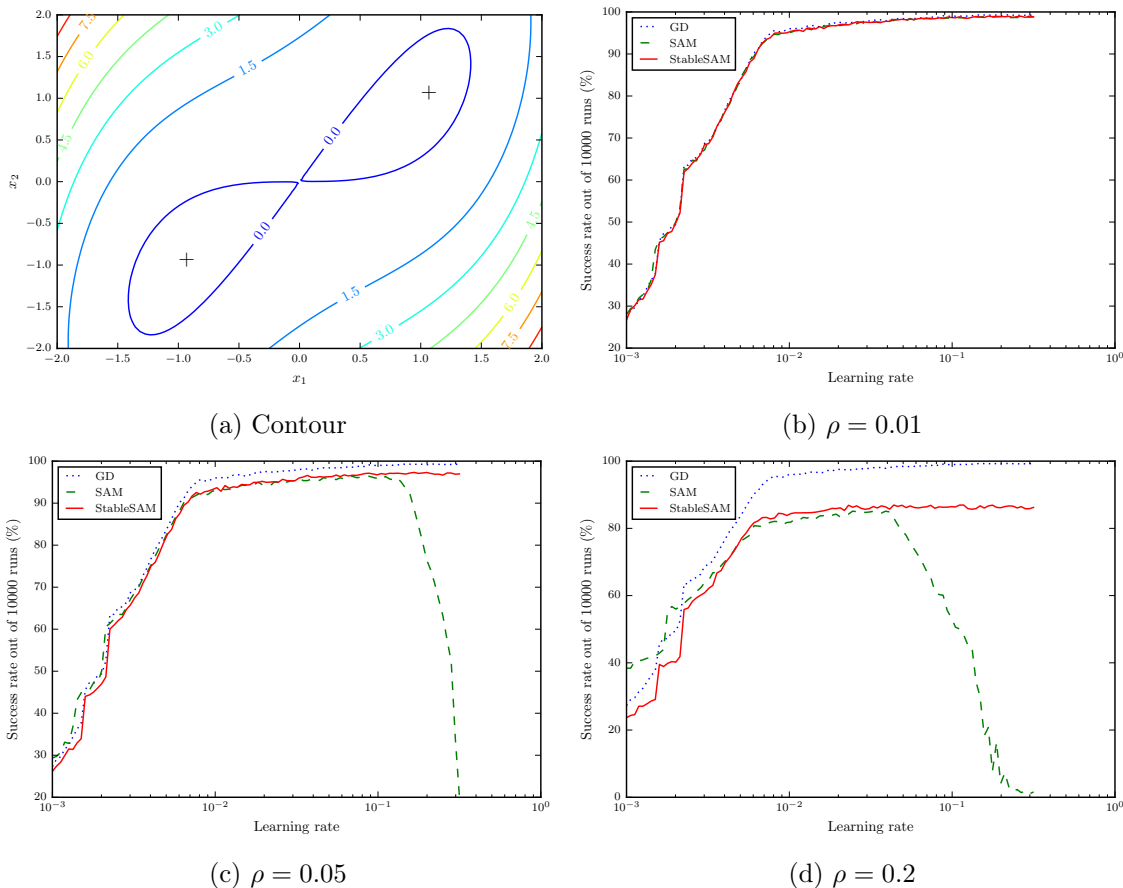


Figure 4: (a) Contour plot of function  $f(x_1, x_2) = x_1^4/4 - x_1x_2 + x_2^2/2$  and the symbol (+) marks the global minima at  $(-1, -1)$  and  $(1, 1)$ , respectively. (b) - (d) exhibit the rate of successful training as a function of the learning rate for different optimizers and perturbation radius  $\rho$ .

### 5.1 Toy Example

Although it is known that SAM can incur instability in training neural networks, a quantitative investigation into this problem is lacking so far. To gain some intuition on how SAM exacerbates the training stability and how StableSAM ameliorates this issue, we consider the following function (Lucchi et al., 2021),

$$f(x_1, x_2) = \frac{1}{4}x_1^4 - x_1x_2 + \frac{1}{2}x_2^2,$$

which has a strict saddle point at  $(0, 0)$  and two global minima at  $(-1, -1)$  and  $(1, 1)$ . Given a starting point, we are interested in whether the training process converges to one of the global minima.

We considered 100 different learning rates that are equispaced between 0.001 and 0.3 on the logarithm scale. For each learning rate, we uniformly sampled 10000 starting points from the square  $[-2, 2] \times [-2, 2]$  and reported the total number of runs that eventually converged

to the global minima. We marked those runs that either get stuck in the saddle point or fail to converge (for example, throw out an exception error) as unsuccessful runs. As shown in Figure 4, gradient descent always achieves the highest rate of successful training. For a relatively large learning rate, approximately larger than 0.1, the possibility of failure drastically increases when trained by SAM. In contrast, this issue can be remedied to a large extent if StableSAM is employed as the learning curve remains approximately constant for large learning rates. It is worth noting that the stability of sharpness-aware training also heavily relies on the perturbation radius  $\rho$ , a fact that both holds for SAM and StableSAM. This is consistent with the intuition that when  $\rho$  is small, the optimization trajectory almost resembles that of gradient descent (see Figure 4b), and when  $\rho$  is large, the deviation from the exact trajectory gradually increases and the training process finally explodes. Another intriguing observation is that the rate of successful training linearly increases for all optimizers in the regime of a small learning rate. This is because they are both likely attracted to the saddle point  $(0, 0)$  when the learning rate is relatively small. As a byproduct, this provides some evidence that a moderately large learning rate is critical to escape from saddle points in training neural networks.

## 5.2 Algorithmic Stability

In Section 4.3, we showed that StableSAM can consistently perform better than SAM in terms of generalization error (see Theorems 8 and 15 for a comparison). To verify this claim empirically, we followed the experimental settings of Hardt et al. (2016) and considered two proxies to measure the algorithmic stability. The first is the normalized Euclidean distance between the parameters of two identical models, namely, with the same architecture and initialization. The second proxy is the generalization error which measures the difference between the training error and the test error.

To construct two training sets  $S$  and  $S'$  that differ in only one example, we first randomly remove an example from the given training set, and the remaining examples naturally constitute one set  $S$ . Then we can create another set  $S'$  by replacing a random example of  $S$  with the one previously deleted. We restricted our attention to the task of image classification and analyzed two different neural architectures: a simple fully connected neural network (FCN) trained on MNIST, and a LeNet (LeCun et al., 1998) trained on CIFAR-10. The FCN model consists of two hidden layers of 500 neurons, each of which is followed by a ReLU activation function. To make our experiments more controllable, we exclude all forms of regularization such as weight decay and dropout. We use the vanilla SGD without momentum acceleration as the default base optimizer and train each model up to 60 epochs with a constant learning rate. Additionally, we do not use data augmentation so that the distribution shift between training data and test data is minimal. Moreover, we record the normalized Euclidean distance and the generalization error once per epoch. It is worth noting that we run each model with three different seeds and only the mean value is plotted as the variation is negligible.

As shown in Figure 5, there is a close correspondence between the normalized parameter distance and the generalization error, which is also verified in Hardt et al. (2016). These two quantities often move in tandem and are positively correlated. Moreover, when starting from the same initialization, models trained by SGD quickly diverge, whereas models trained

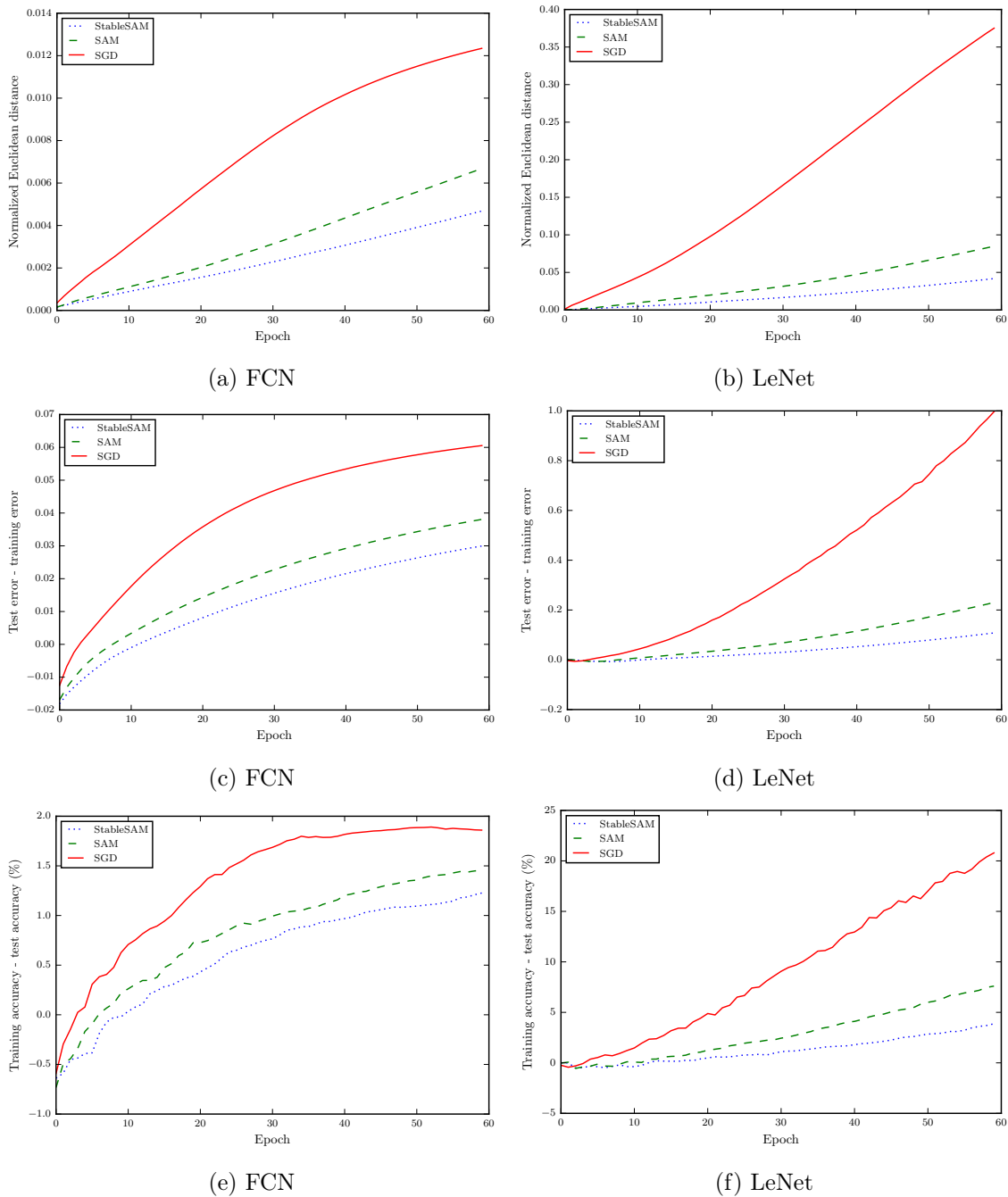
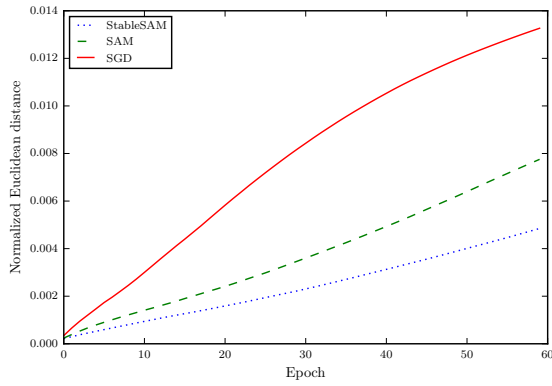
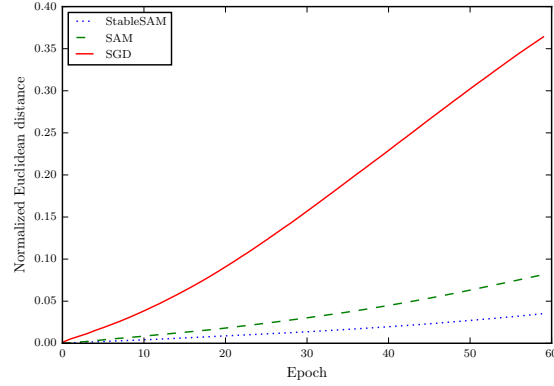


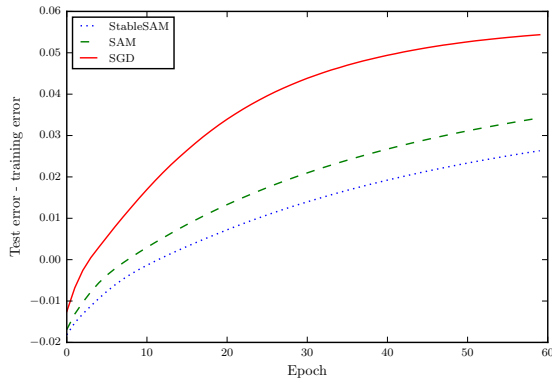
Figure 5: Evolution of different metrics on measuring the algorithmic stability of SGD, SAM, and StableSAM. The left panel depicts the results of training a fully connected neural network on MNIST and the right panel depicts the results of training a LeNet on CIFAR-10. All models are trained up to 60 epochs with a constant learning rate and neither momentum nor weight decay is employed.



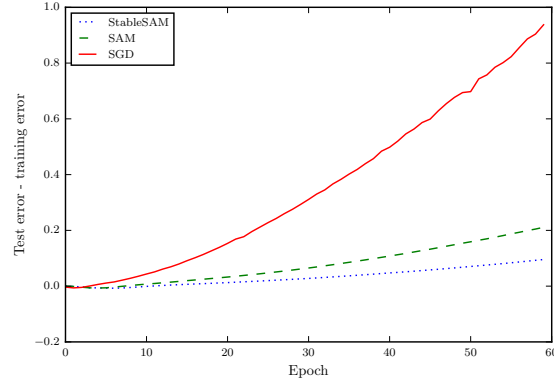
(a) FCN



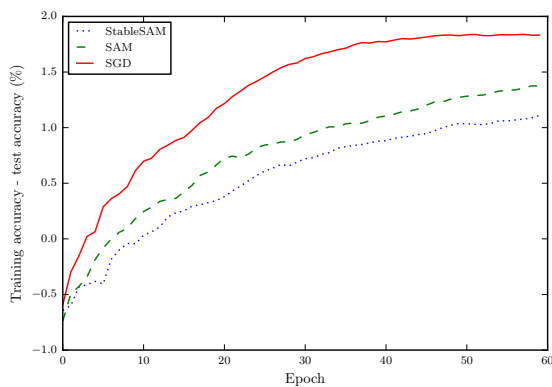
(b) LeNet



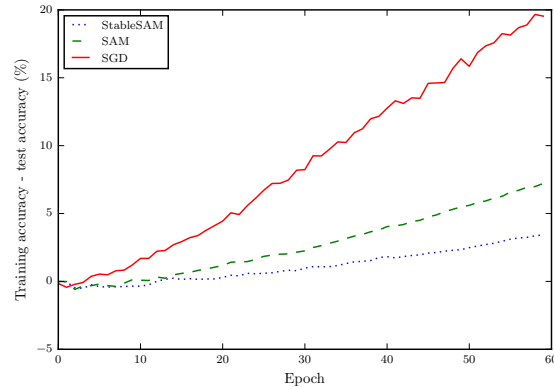
(c) FCN



(d) LeNet



(e) FCN



(f) LeNet

Figure 6: Evolution of different metrics on measuring the algorithmic stability of SGD, SAM, and StableSAM. The left panel depicts the results of training a fully connected neural network on MNIST and the right panel depicts the results of training a LeNet on CIFAR-10. All models are trained up to 60 epochs with a constant learning rate and a weight decay of  $5.0e-4$  is employed.

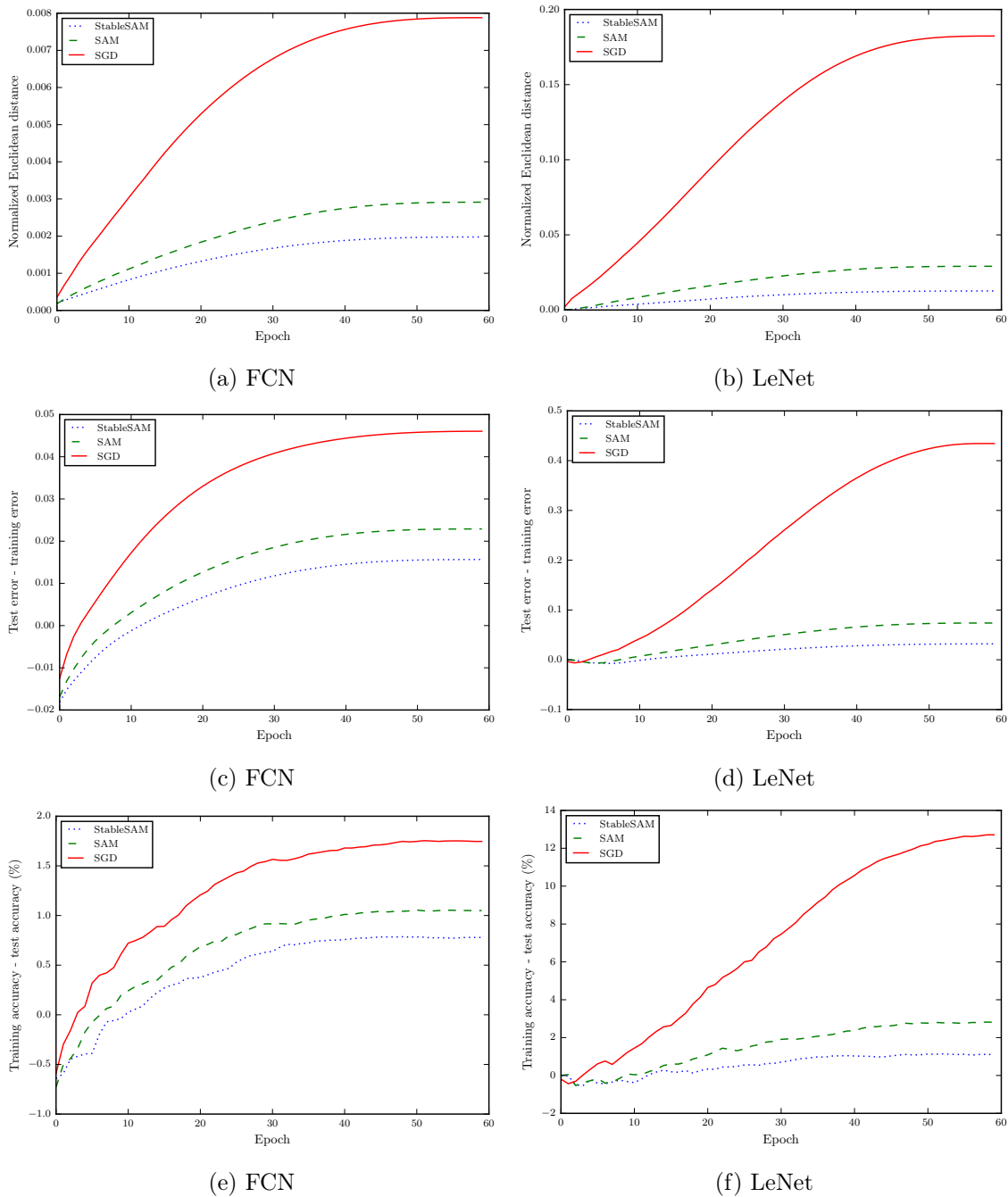


Figure 7: Evolution of different metrics on measuring the algorithmic stability of SGD, SAM, and StableSAM. The left panel depicts the results of training a fully connected neural network on MNIST and the right panel depicts the results of training a LeNet on CIFAR-10. All models are trained up to 60 epochs and the learning rate is decayed with a cosine schedule.

Table 2: Results on CIFAR-10 and CIFAR-100. We run each model with three different random seeds and report the mean test accuracy (%) along with the standard deviation. Text marked as bold indicates the best result.

		SGD	SAM	StableSAM	ASAM	StableASAM
CIFAR-10	ResNet-20	93.01 ± 0.16	93.68 ± 0.12	<b>93.95 ± 0.08</b>	93.73 ± 0.06	93.77 ± 0.09
	ResNet-56	94.22 ± 0.05	95.37 ± 0.12	<b>95.68 ± 0.09</b>	95.21 ± 0.12	95.18 ± 0.04
	ResNext-29-32x4d	95.71 ± 0.06	96.47 ± 0.11	<b>96.94 ± 0.06</b>	96.55 ± 0.13	96.45 ± 0.15
	WRN-28-10	96.11 ± 0.04	<b>97.11 ± 0.04</b>	97.02 ± 0.01	97.01 ± 0.15	97.04 ± 0.01
	PyramidNet-110	96.24 ± 0.05	<b>97.42 ± 0.08</b>	97.37 ± 0.12	97.19 ± 0.11	97.23 ± 0.02
CIFAR-100	ResNet-20	69.71 ± 0.27	71.19 ± 0.18	71.42 ± 0.23	<b>71.51 ± 0.28</b>	71.32 ± 0.09
	ResNet-56	72.50 ± 0.18	76.01 ± 0.21	<b>76.31 ± 0.14</b>	75.90 ± 0.34	76.16 ± 0.09
	ResNext-29-32x4d	80.89 ± 0.23	82.32 ± 0.08	<b>82.71 ± 0.13</b>	82.44 ± 0.11	82.57 ± 0.23
	WRN-28-10	80.99 ± 0.19	83.73 ± 0.07	<b>83.78 ± 0.12</b>	83.50 ± 0.14	83.58 ± 0.19
	PyramidNet-110	81.85 ± 0.31	84.53 ± 0.19	<b>84.61 ± 0.33</b>	83.62 ± 0.54	83.84 ± 0.23

by SAM and StableSAM change slowly. By comparing the training curves, we can further observe that StableSAM is significantly less sensitive than SAM when the training set is modified. Instead of the generalization error, when we measure the disparity between the training accuracy and the test accuracy, we can still observe the same changing trend. Surprisingly, when we trained the models using weight decay or a decaying learning rate, we still observed a similar changing trend (see Figures 6 and 7).

### 5.3 Image Classification from Scratch

In this section, we apply the renormalization strategy on SAM and ASAM (Kwon et al., 2021) and investigate its influence on the final generalization performance when models are trained from scratch on two typical image classification problems. For notational simplicity, we refer to the optimizer that applies the renormalization strategy on ASAM as StableASAM.

**CIFAR-10 and CIFAR-100 (Krizhevsky et al., 2009).** We considered several popular backbones, ranging from basic ResNets (He et al., 2016) to more advanced architectures such as WideResNet (Zagoruyko and Komodakis, 2016), ResNeXt (Xie et al., 2017), and PyramidNet (Han et al., 2017). To increase reproductivity, we used standard implementations of these architectures that are encapsulated in a Pytorch package<sup>3</sup>. Beyond basic data augmentation such as horizontal flip, random crop, and normalization, we only used label smoothing (Müller et al., 2019) with a factor of 0.1. We used a constant mini-batch size of 128 and each model was trained up to 200 epochs with a cosine learning rate decay (Loshchilov and Hutter, 2016). The default base optimizer is SGD with a momentum of 0.9. Following Kwon et al. (2021); Kim et al. (2022), we only tuned the perturbation radius  $\rho$ , and the learning rate and the coefficient of weight decay defaulted to be 0.1 and 5.0e-4. For SAM and StableSAM, we swept the perturbation radius  $\rho$  over  $\{0.01, 0.02, 0.05, 0.1, 0.2\}$ . For ASAM and StableASAM, as suggested by Kwon et al. (2021), the perturbation radius  $\rho$  needs to be much larger, and we ranged it from  $\{0.1, 0.2, 0.5, 1.0, 2.0\}$ . We ran each model

3. Details can be found at <https://pypi.org/project/pytorchcv>.



Table 3: Top-1 accuracy (%) on ImageNet-1k with Inception-style data augmentation only. The base optimizer for ResNets is SGD with momentum 0.9 and each model is trained for 90 epochs. In contrast, the base optimizer for ViT is AdamW and each model is trained up to 300 epochs.

	SGD/AdamW	SAM	StableSAM	ASAM	StableASAM
ResNet-50	77.0	77.2	<b>77.6</b>	77.3	77.5
ResNet-101	77.9	78.9	<b>79.1</b>	78.9	79.0
ResNet-152	78.4	80.0	<b>80.1</b>	79.7	79.8
ViT-S/32	68.1	70.3	<b>70.6</b>	69.2	69.4

with three different random seeds and reported the mean and the standard deviation of the best accuracy on the test set.

Compared to SAM and ASAM, Table 2 suggests that the renormalization strategy essentially can further boost the generalization performance and the improvement is more pronounced on the CIFAR-100 data set. For example, ResNet-56 only attains a test accuracy of 76.01% when trained by SAM, but the accuracy increases to 76.31% after the renormalization strategy is applied.

**ImageNet-1k (Deng et al., 2009).** To investigate the performance of the renormalization strategy on a larger scale, we further evaluated it with the ImageNet-1k data set. We only used basic data augmentations, namely, resizing and cropping images to 224-pixel resolution and then normalizing them. We considered several typical architectures<sup>4</sup>, including ResNet-50, ResNet-101, ResNet-152, and Vision Transformer (ViT) (Dosovitskiy et al., 2021). For ResNets, models are trained only for 90 epochs and the default base optimizer is SGD with momentum acceleration. The peak learning rate is 0.1 and the weight decay coefficient is 1.0e-4. According to Foret et al. (2021); Kwon et al. (2021), the perturbation radius  $\rho$  for SAM and StableSAM is set to be 0.05 and 1.0 for ASAM and StableASAM. For ViT, the model is trained up to 300 epochs and the default base optimizer is changed to AdamW. The peak learning rate is 3.0e-4 and the weight decay is 0.3. Since ViT favors larger  $\rho$  than ResNet does (Chen et al., 2022), we set  $\rho$  of SAM and StableSAM to be 0.2 and 2.0 for ASAM and StableASAM accordingly. For both models, we used a constant mini-batch size of 256, and the cosine learning rate decay schedule was also employed. As shown in Table 3, the renormalization strategy remains effective on the ImageNet-1k data set. After applying the renormalization strategy to SAM and ASAM, we can observe an improved top-1 accuracy for all models, though the improvement is more pronounced for SAM than for ASAM.

#### 5.4 Robustness to Shuffled Label

In previous works, including Foret et al. (2021); Kwon et al. (2021); Kim et al. (2022), both approaches are shown to be robust to random label noise in the training set. Similar to their experiments, we also shuffled the labels by random flipping with different proportions (20%,

4. Both models are trained with the timm library that is available at <https://github.com/huggingface/pytorch-image-models>.

Table 4: Maximum test accuracy when models are trained on CIFAR-10 with random label noise. At each iteration, the input features remain not touched, whilst the labels are proportionally shuffled.

Noise Level	ResNet-56		WRN-28-10	
	SAM	StableSAM	SAM	StableSAM
20%	94.52 $\pm$ 0.11	<b>94.73 <math>\pm</math> 0.07</b>	96.62 $\pm$ 0.04	<b>96.64 <math>\pm</math> 0.08</b>
40%	93.92 $\pm$ 0.09	<b>94.03 <math>\pm</math> 0.02</b>	96.29 $\pm$ 0.02	<b>96.47 <math>\pm</math> 0.04</b>
60%	91.57 $\pm$ 0.08	<b>91.66 <math>\pm</math> 0.06</b>	95.38 $\pm$ 0.03	<b>95.42 <math>\pm</math> 0.21</b>
80%	79.42 $\pm$ 0.95	<b>80.71 <math>\pm</math> 0.57</b>	87.38 $\pm$ 0.19	<b>87.53 <math>\pm</math> 0.34</b>

40%, 60%, and 80%). We then trained ResNet-56 and WRN-28-10 on the corrupted CIFAR-10 data set with SAM and StableSAM. For both models, we used a constant mini-batch size of 128 as before and we fixed the perturbation radius  $\rho$  to be 0.05. Both the learning rate and the weight decay coefficient followed the same setting as in Section 5.3. Each model was trained with three different random seeds and we finally reported the mean and the standard deviation of the maximum accuracy on the test set. As illustrated by Table 4, the results suggest that StableSAM consistently performs better than SAM for both models, indicating that the renormalization strategy is beneficial to enhance the test accuracy across various noise levels.

## 6. Conclusion

In this paper, we proposed a renormalization strategy to mitigate the issue of instability in sharpness-aware training. We also evaluated its efficacy, both theoretically and empirically. Following this line, we believe several directions deserve further investigation. Although we have verified that StableSAM and SAM both can greatly improve the generalization performance over SGD, it remains unknown whether they converge to the same attractor of minima, properties of which might significantly differ from those found by SGD (Kadour et al., 2022). Besides, probing to what extent the renormalization strategy reshapes the optimization trajectory or the scope of the parameter space it explores is also of interest. Another intriguing direction involves controlling the renormalization factor during the training process, for example, by imposing explicit constraints on its bounds or adjusting the perturbation radius according to the norm of the exact gradient. Finally, the influence of renormalization strategy on adversarial robustness should also be investigated (Wei et al., 2023).

## Acknowledgments

This work was supported in part by the National Key Research and Development Program of China under Grant 2020AAA0105601 and in part by the National Natural Science Foundation of China under Grants 61976174, 62276208.

## References

- Maksym Andriushchenko and Nicolas Flammarion. Towards understanding sharpness-aware minimization. In *Proceedings of the 43rd International Conference on Machine Learning*, pages 639–668, 2022.
- Dara Bahri, Hossein Mobahi, and Yi Tay. Sharpness-aware minimization improves language model generalization. In *Proceedings of the 60th Annual Meeting of the Association for Computational Linguistics*, volume 1, pages 7360–7371, 2022.
- Peter L Bartlett, Philip M Long, and Olivier Bousquet. The dynamics of sharpness-aware minimization: Bouncing across ravines and drifting towards wide minima. *Journal of Machine Learning Research*, 24(316):1–36, 2023.
- Devansh Bisla, Jing Wang, and Anna Choromanska. Low-pass filtering SGD for recovering flat optima in the deep learning optimization landscape. In *Proceedings of the 25th International Conference on Artificial Intelligence and Statistics*, pages 8299–8339, 2022.
- Léon Bottou, Frank E Curtis, and Jorge Nocedal. Optimization methods for large-scale machine learning. *SIAM Review*, 60(2):223–311, 2018.
- Olivier Bousquet and André Elisseeff. Stability and generalization. *The Journal of Machine Learning Research*, 2:499–526, 2002.
- Sébastien Bubeck et al. Convex optimization: Algorithms and complexity. *Foundations and Trends® in Machine Learning*, 8(3-4):231–357, 2015.
- Pratik Chaudhari, Anna Choromanska, Stefano Soatto, Yann LeCun, Carlo Baldassi, Christian Borgs, Jennifer Chayes, Levent Sagun, and Riccardo Zecchina. Entropy-SGD: Biasing gradient descent into wide valleys. *Journal of Statistical Mechanics: Theory and Experiment*, 2019(12):124018, 2019.
- Xiangning Chen, Cho-Jui Hsieh, and Boqing Gong. When vision Transformers outperform Resnets without pretraining or strong data augmentations. In *Proceedings of the 10th International Conference on Learning Representations*, pages 1–20, 2022.
- Dami Choi, Christopher J Shallue, Zachary Nado, Jaehoon Lee, Chris J Maddison, and George E Dahl. On empirical comparisons of optimizers for deep learning. *arXiv preprint arXiv:1910.05446*, 2019.
- Enea Monzio Compagnoni, Luca Biggio, Antonio Orvieto, Frank Norbert Proske, Hans Kersting, and Aurelien Lucchi. An SDE for modeling SAM: Theory and insights. In *Proceedings of the 44th International Conference on Machine Learning*, pages 25209–25253, 2023.
- George E Dahl, Frank Schneider, Zachary Nado, Naman Agarwal, Chandramouli Shama Sastry, Philipp Hennig, Sourabh Medapati, Runa Eschenhagen, Priya Kasimbeg, Daniel Suo, et al. Benchmarking neural network training algorithms. *arXiv preprint arXiv:2306.07179*, 2023.

- Zihang Dai, Zhilin Yang, Yiming Yang, Jaime G Carbonell, Quoc Le, and Ruslan Salakhutdinov. Transformer-XL: Attentive language models beyond a fixed-length context. In *Proceedings of the 57th Annual Meeting of the Association for Computational Linguistics*, pages 2978–2988, 2019.
- Alex Davies, Petar Veličković, Lars Buesing, Sam Blackwell, Daniel Zheng, Nenad Tomašev, Richard Tanburn, Peter Battaglia, Charles Blundell, András Juhász, et al. Advancing mathematics by guiding human intuition with AI. *Nature*, 600(7887):70–74, 2021.
- Jia Deng, Wei Dong, Richard Socher, Li-Jia Li, Kai Li, and Li Fei-Fei. Imagenet: A large-scale hierarchical image database. In *Proceedings of the 25th IEEE/CVF Conference on Computer Vision and Pattern Recognition*, pages 248–255, 2009.
- Alexey Dosovitskiy, Lucas Beyer, Alexander Kolesnikov, Dirk Weissenborn, Xiaohua Zhai, Thomas Unterthiner, Mostafa Dehghani, Matthias Minderer, Georg Heigold, Sylvain Gelly, et al. An image is worth 16x16 words: Transformers for image recognition at scale. In *Proceedings of the International Conference on Learning Representations*, pages 1–21, 2021.
- Jiawei Du, Hanshu Yan, Jiashi Feng, Joey Tianyi Zhou, Liangli Zhen, Rick Siow Mong Goh, and Vincent Tan. Efficient sharpness-aware minimization for improved training of neural networks. In *Proceedings of the 10th International Conference on Learning Representations*, pages 1–18, 2022a.
- Jiawei Du, Daquan Zhou, Jiashi Feng, Vincent Tan, and Joey Tianyi Zhou. Sharpness-aware training for free. In *Proceedings of the 36th Conference on Neural Information Processing Systems*, volume 35, pages 23439–23451, 2022b.
- John Duchi, Elad Hazan, and Yoram Singer. Adaptive subgradient methods for online learning and stochastic optimization. *Journal of Machine Learning Research*, 12(7), 2011.
- Pierre Foret, Ariel Kleiner, Hossein Mobahi, and Behnam Neyshabur. Sharpness-aware minimization for efficiently improving generalization. In *Proceedings of the 9th International Conference on Learning Representations*, pages 1–20, 2021.
- Dongyoon Han, Jiwhan Kim, and Junmo Kim. Deep pyramidal residual networks. In *Proceedings of the 33rd IEEE/CVF Conference on Computer Vision and Pattern Recognition*, pages 5927–5935, 2017.
- Moritz Hardt, Ben Recht, and Yoram Singer. Train faster, generalize better: Stability of stochastic gradient descent. In *Proceedings of the 37th International Conference on Machine Learning*, pages 1225–1234, 2016.
- Kosuke Haruki, Taiji Suzuki, Yohei Hamakawa, Takeshi Toda, Ryuji Sakai, Masahiro Ozawa, and Mitsuhiro Kimura. Gradient noise convolution: Smoothing loss function for distributed large-batch SGD. *arXiv preprint arXiv:1906.10822*, 2019.
- Fengxiang He, Tongliang Liu, and Dacheng Tao. Control batch size and learning rate to generalize well: Theoretical and empirical evidence. In *Proceedings of 33rd Conference on Neural Information Processing Systems*, volume 32, pages 1–10, 2019.

- Kaiming He, Xiangyu Zhang, Shaoqing Ren, and Jian Sun. Deep residual learning for image recognition. In *Proceedings of the 32nd IEEE Conference on Computer Vision and Pattern Recognition*, pages 770–778, 2016.
- Geoffrey E Hinton and Drew van Camp. Keeping neural networks simple. In *Proceedings of the International Conference on Artificial Neural Networks*, pages 11–18, 1993.
- Stanisław Jastrzebski, Zachary Kenton, Devansh Arpit, Nicolas Ballas, Asja Fischer, Yoshua Bengio, and Amos Storkey. Three factors influencing minima in SGD. *Artificial Neural Networks and Machine Learning*, pages 1–14, 2018.
- John Jumper, Richard Evans, Alexander Pritzel, Tim Green, Michael Figurnov, Olaf Ronneberger, Kathryn Tunyasuvunakool, Russ Bates, Augustin Žídek, Anna Potapenko, et al. Highly accurate protein structure prediction with AlphaFold. *Nature*, 596(7873):583–589, 2021.
- Jean Kaddour, Linqing Liu, Ricardo Silva, and Matt J Kusner. When do flat minima optimizers work? In *Proceedings of the 36th Conference on Neural Information Processing Systems*, volume 35, pages 16577–16595, 2022.
- Nitish Shirish Keskar, Dheevatsa Mudigere, Jorge Nocedal, Mikhail Smelyanskiy, and Ping Tak Peter Tang. On large-batch training for deep learning: Generalization gap and sharp minima. In *Proceedings of the 5th International Conference on Learning Representations*, pages 1–16, 2017.
- Hoki Kim, Jinseong Park, Yujin Choi, and Jaewook Lee. Stability analysis of sharpness-aware minimization. *arXiv preprint arXiv:2301.06308*, 2023.
- Minyoung Kim, Da Li, Shell X Hu, and Timothy Hospedales. Fisher SAM: Information geometry and sharpness aware minimisation. In *Proceedings of the 43rd International Conference on Machine Learning*, pages 11148–11161, 2022.
- Diederik P Kingma and Jimmy Ba. Adam: A method for stochastic optimization. *arXiv preprint arXiv:1412.6980*, 2014.
- Alex Krizhevsky, Geoffrey Hinton, et al. Learning multiple layers of features from tiny images. Technical report, University of Toronto, 2009.
- Jungmin Kwon, Jeongseop Kim, Hyunseo Park, and In Kwon Choi. ASAM: Adaptive sharpness-aware minimization for scale-invariant learning of deep neural networks. In *Proceedings of the 42nd International Conference on Machine Learning*, pages 5905–5914, 2021.
- Yann LeCun, Léon Bottou, Yoshua Bengio, and Patrick Haffner. Gradient-based learning applied to document recognition. *Proceedings of the IEEE*, 86(11):2278–2324, 1998.
- Bingcong Li and Georgios B Giannakis. Enhancing sharpness-aware optimization through variance suppression. *arXiv preprint arXiv:2309.15639*, 2023.

- Yong Liu, Siqu Mai, Xiangning Chen, Cho-Jui Hsieh, and Yang You. Towards efficient and scalable sharpness-aware minimization. In *Proceedings of the 38th IEEE/CVF Conference on Computer Vision and Pattern Recognition*, pages 12360–12370, 2022a.
- Yong Liu, Siqu Mai, Minhao Cheng, Xiangning Chen, Cho-Jui Hsieh, and Yang You. Random sharpness-aware minimization. In *Proceedings of the 36th Conference on Neural Information Processing Systems*, volume 35, pages 24543–24556, 2022b.
- Ilya Loshchilov and Frank Hutter. SGDR: Stochastic gradient descent with warm restarts. *arXiv preprint arXiv:1608.03983*, 2016.
- Aurelien Lucchi, Antonio Orvieto, and Adamos Solomou. On the second-order convergence properties of random search methods. In *Proceedings of the 35th Conference on Neural Information Processing Systems*, volume 34, pages 25633–25645, 2021.
- Stephan Mandt, Matthew D Hoffman, and David M Blei. Stochastic gradient descent as approximate Bayesian inference. *Journal of Machine Learning Research*, 18:1–35, 2017.
- Peng Mi, Li Shen, Tianhe Ren, Yiyi Zhou, Xiaoshuai Sun, Rongrong Ji, and Dacheng Tao. Make sharpness-aware minimization stronger: A sparsified perturbation approach. In *Proceedings of the 36th Conference on Neural Information Processing Systems*, volume 35, pages 30950–30962, 2022.
- Rafael Müller, Simon Kornblith, and Geoffrey E Hinton. When does label smoothing help? In *Proceedings of the 33rd Conference on Neural Information Processing Systems*, volume 32, pages 1–13, 2019.
- Renkun Ni, Ping-yeh Chiang, Jonas Geiping, Micah Goldblum, Andrew Gordon Wilson, and Tom Goldstein. K-SAM: Sharpness-aware minimization at the speed of SGD. *arXiv preprint arXiv:2210.12864*, 2022.
- Joseph Redmon, Santosh Divvala, Ross Girshick, and Ali Farhadi. You only look once: Unified, real-time object detection. In *Proceedings of the 31st IEEE/CVF Conference on Computer Vision and Pattern Recognition*, pages 779–788, 2016.
- Zeming Wei, Jingyu Zhu, and Yihao Zhang. Sharpness-aware minimization alone can improve adversarial robustness. In *New Frontiers in Adversarial Machine Learning Workshop of the 40th International Conference on Machine Learning*, pages 1–12, 2023.
- Kaiyue Wen, Tengyu Ma, and Zhiyuan Li. How does sharpness-aware minimization minimize sharpness? In *Optimization for Machine Learning Workshop of 35th Conference on Neural Information Processing Systems*, pages 1–94, 2022.
- Ashia C Wilson, Rebecca Roelofs, Mitchell Stern, Nati Srebro, and Benjamin Recht. The marginal value of adaptive gradient methods in machine learning. In *Proceedings of 31st Conference on Neural Information Processing Systems*, volume 30, pages 1–10, 2017.
- Lei Wu, Chao Ma, et al. How SGD selects the global minima in over-parameterized learning: A dynamical stability perspective. In *Proceedings of the 32nd Conference on Neural Information Processing Systems*, volume 31, pages 1–10, 2018.

- Saining Xie, Ross Girshick, Piotr Dollár, Zhuowen Tu, and Kaiming He. Aggregated residual transformations for deep neural networks. In *Proceedings of the 33rd IEEE/CVF Conference on Computer Vision and Pattern Recognition*, pages 1492–1500, 2017.
- Zhewei Yao, Amir Gholami, Kurt Keutzer, and Michael W Mahoney. Pyhessian: Neural networks through the lens of the Hessian. In *Proceedings of the IEEE International Conference on Big Data*, pages 581–590, 2020.
- Yun Yue, Jiadi Jiang, Zhiling Ye, Ning Gao, Yongchao Liu, and Ke Zhang. Sharpness-aware minimization revisited: Weighted sharpness as a regularization term. In *Proceedings of the 29th ACM SIGKDD Conference on Knowledge Discovery and Data Mining*, pages 1–10, 2023.
- Sergey Zagoruyko and Nikos Komodakis. Wide residual networks. *arXiv preprint arXiv:1605.07146*, 2016.
- Xingxuan Zhang, Renzhe Xu, Han Yu, Hao Zou, and Peng Cui. Gradient norm aware minimization seeks first-order flatness and improves generalization. In *Proceedings of the 39th IEEE/CVF Conference on Computer Vision and Pattern Recognition*, pages 20247–20257, 2023.
- Zhiyuan Zhang, Ruixuan Luo, Qi Su, and Xu Sun. GA-SAM: Gradient-strength based adaptive sharpness-aware minimization for improved generalization. In *Proceedings of the Conference on Empirical Methods in Natural Language Processing*, pages 3888–3903, 2022.
- Yang Zhao, Hao Zhang, and Xiuyuan Hu. Penalizing gradient norm for efficiently improving generalization in deep learning. In *Proceedings of the 43rd International Conference on Machine Learning*, pages 26982–26992, 2022a.
- Yang Zhao, Hao Zhang, and Xiuyuan Hu. Randomized sharpness-aware training for boosting computational efficiency in deep learning. *arXiv preprint arXiv:2203.09962*, 2022b.
- Pan Zhou, Jiashi Feng, Chao Ma, Caiming Xiong, Steven Chu Hong Hoi, et al. Towards theoretically understanding why SGD generalizes better than Adam in deep learning. In *Proceedings of 34th Conference on Neural Information Processing Systems*, volume 33, pages 21285–21296, 2020.
- Wenxuan Zhou, Fangyu Liu, Huan Zhang, and Muhao Chen. Sharpness-aware minimization with dynamic reweighting. In *Findings of the Association for Computational Linguistics*, pages 5686–5699, 2022.
- Yixuan Zhou, Yi Qu, Xing Xu, and Hengtao Shen. ImbSAM: A closer look at sharpness-aware minimization in class-imbalanced recognition. In *Proceedings of the 39th IEEE/CVF International Conference on Computer Vision*, pages 11345–11355, 2023.
- Juntang Zhuang, Boqing Gong, Liangzhe Yuan, Yin Cui, Hartwig Adam, Nicha C Dvornek, James s Duncan, Ting Liu, et al. Surrogate gap minimization improves sharpness-aware training. In *Proceedings of the 10th International Conference on Learning Representations*, pages 1–24, 2022.